Geomechanics for Energy and the Environment 28 (2021) 100252

Contents lists available at ScienceDirect

Geomechanics for Energy and the Environment

journal homepage: www.elsevier.com/locate/gete

Critical review of wellbore ballooning and breathing literature

Silvio Baldino [a,*], Meng Meng [b]

[a] The University of Tulsa, Tulsa, OK, USA
[b] EES-14, Los Alamos National Laboratory, Los Alamos, NM, USA

ARTICLE INFO

Article history:
Received 1 December 2020
Received in revised form 31 March 2021
Accepted 1 April 2021
Available online 6 April 2021

Editors-in-Chief:
Professor Lyesse Laloui and Professor Tomasz Hueckel

Keywords:
Wellbore breathing
Wellbore ballooning
Loss and gains
Review paper

ABSTRACT

Reversible drilling fluid losses are a major concern of many drilling operations. They alternate fluid losses to fluid returns, the latter representing an unexpected influx to the wellbore. The phenomenon is generally referred to as wellbore ballooning or breathing, and its correct interpretation is paramount for two main reasons. (1) Misinterpretation may jeopardize kick detection operations and lead to kick misdiagnosis. If a kick is wrongly assumed to be a mudflow return, such a scenario could result in well unloading. (2) On the other hand, potential safety issues can also derive from attempts to kill a breathing well when a kick is incorrectly diagnosed. Undermining of wellbore integrity and increments of Non-Productive Time (NPT) are the resulting consequences of the unnecessary implementation of well-control practices. In this paper, references in the literature are examined. Special emphasis is given to critically evaluate the proposed theoretical models. In addition, industry approaches and remedies to wellbore ballooning/breathing are also reviewed.

1. Introduction

The terms *ballooning* and *breathing* of a wellbore are commonly used to describe reversible drilling fluid losses during circulation, followed by fluid regains of comparable amount when circulation is stopped. Because no flow is expected to occur during pumps-off periods, the mudflow return is more noticeable. The implication is therefore clear: wellbore ballooning or breathing may jeopardize reservoir fluid influx (kick) detection operations and lead to kick misdiagnosis. This fact inevitably captures the attention, and however it might be wished otherwise, prompts challenging questions. Are all the wells susceptible to wellbore ballooning/breathing? Is there a way to identify this phenomenon during real time operations? If identified, what are the most practical steps to contain it[1]? To date, both industry and the scientific community have bestowed a considerable effort to properly address the aforementioned phenomenon and increase understanding of its physical characterization. A study of why wellbore ballooning/breathing occurs should begin with a clear picture of the mechanisms behind it. During the years, several explanations have been proposed to resolve the nature of mudflow return when drilling fluid circulation is halted. However, it is difficult always to determine the starting date of a particular field of research, as its applications might have differed from the one related to this particular subject. Moreover, different explanations were investigated during the same period. For this reason, the brief discussion that follows (and the more detailed investigation of the subsequent section) will be temporally eclectic, chronologically consistent insofar as possible, but concerned more with the proposed physical explanations rather than with the dates of publication. In the late Eighty's, Gill[2,3,4] described and collected a significant number of field observations, based on which he proposed his explanation for the recorded mud loss/gain events. Accordingly, elastic deformation of the borehole walls was considered the main mechanism behind the reversible losses, and the term *ballooning shale* was coined. More specifically, high wellbore pressure would result in the increase of borehole volume, whilst lower pressures would cause volume reduction, hence mud loss and gain respectively (especially noticeable while drilling soft shale formations). The very same concept was further investigated by other authors, including Helstrup et al.[5] The thermal volumetric changes experienced by the drilling fluid have been also accounted for as a reason behind fluid gains and losses.[6,7] Ultimately, a quite remarkable effort has been made to describe borehole breathing resulting from the hydraulic interaction between wellbore and fractured formation. The fluid progressively flows in and out of fractures as a consequence of the pressure fluctuations occurring at each circulation cycle. Besides the mentioned causes, fracture aperture variations should play a major role while drilling in fractured formations.[8–10] In parallel to the developments of the scientific community, industry has been playing a prominent role in the attempt to describe the nature of the loss and gain events, and to propose the most practical steps to manage it. The number of published studies related to

* Now at Shell International Exploration and Production, Houston, TX, USA. Correspondence to: silvio-baldino@utulsa.edu (S. Baldino)
E-mail address: silvio-baldino@utulsa.edu (S. Baldino).

https://doi.org/10.1016/j.gete.2021.100252
2352-3808/

ballooning/breathing wells is most impressive, and many are the techniques that have been implemented in the field to deal with the issue. Each and every technique undoubtedly represents a fascinating topic that offers a tempting diversion from the present work. It is a diversion that will largely have to be resisted. It cannot be wholly resisted, for borehole ballooning/breathing may not be understood except in the context of how its practical fingerprinting and remedies function and operate. Accordingly, industry's approaches and remedies will be treated in only a partial fashion.

1.1. Framework of discussion

The goal of this study throughout is to look at borehole ballooning/breathing as a general phenomenon in order to gain an understanding, not limited to specific cases, but applicable across a wide range of drilling environments. The premise of this review approach is that if the logic of an argument is faulty, a discussion of factual matters is largely unnecessary. If the elastic deformation of the borehole walls or the fluid thermal expansion could not have caused the generally recorded magnitude and signature of loss/gain events, then all the evidence for or against these is interesting, but immaterial. Hence, in what follows the major focus will be on the logic of proposed explanations. Factual matters will be discussed but are not of major importance. Finally, the stimulus to undertake this study was the spread perception that some of the existing explanations of ballooning/breathing logically cannot account for it.[11,12] The next sections will detail the reservations about published approaches and show where these approaches fail. The tone is necessarily critical, but it is worth noting that for all this, the existing literature does have much to offer in understanding ballooning/breathing. After these pages of constructive criticism, the final section will conclude with summarizing comments.

1.2. Classification of theories

The diversity of views behind loss/gain events dictates a need to impose order. As previously mentioned, most of the theories fall into a limited number of recurrent explanatory themes. These themes, by and large, persisted through time. The authors whose works are here assigned to each theme are characterized by overriding similarities in framework, assumptions, and approach. Within each theme, of course, a great deal of diversity still exists, so that some level of individual discussion is necessary for many authors. Any good classifier knows that in the process of classification, information about variety is lost while information about similarities is gained. The utility of a classification must be judged (at least partially) by whether the quantity and quality of information gained outweighs that lost, and this depends largely on the purposes and needs of the analyst. In some respects, subdivision in physical mechanisms behind ballooning /breathing is useful in that it facilitates initial communication and comparison. Yet in this particular review work, some of the weaknesses of the typological approach become apparent. The degree of variation among proposed models, such as for breathing in fractured formations, is such that many could feel uncomfortable with the concept (e.g. single fracture approach, continuum approach, and inclusion of poroelastic effects). For many purposes, it may obscure more than it reveals. Solutions that focus on further subdividing each single physical mechanisms bring only the potential for endless debate, and unprofitable concentration on labels rather than on processes of loss and gain. Therefore, the typological distinction of most interest here is the one which exists between the location of origin of the loss/gain event, namely internally to the well (wellbore walls included), or externally (i.e. in the adjacent formation). In the next sections, three major topics will then be addressed: (1) internal causes, (2) external causes, and (3) industry approaches and remedies. The discussion that follows will be necessarily selective, focusing on those aspects of the proposed models that are relevant to understanding ballooning/breathing.

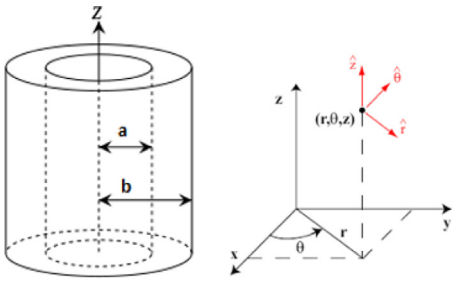

Fig. 1. Thick walled cylinder schematic view.

1.3. Natural vs. Induced fractures

Among the reviewed works that look at fractures as the main cause of loss/gain events, the contribution of drilling induced fractures is seldom analyzed or distinguished. Most of the authors that will be presented, looked at non-propagating natural fractures, and in some isolated cases the propagation of already existing fractures will be accounted for. However, the impact that hydraulic fractures have on wellbore breathing could be significant. Not all formations are naturally fractured, especially with natural fractures that are conductive. Sometimes the wellbore pressure that can initiate and grow a new induced fracture is lower than the pressure required to open pre-existing natural fractures (due to their unfavorable orientation relative to the stress field). To the authors' knowledge, the mechanism of wellbore breathing through hydraulically induced fractures has not been treated yet, except for Maury and Idelovici[13], where full focus is on opening and closing of induced fractures downhole. Accordingly, loss and gains were attributed to:

- Strength reduction of the formation caused by fracture initiation by cooling of the formation during circulation.
- Further fracture propagation due to continued cooling, coupled with increasing mud weights.

Unless clearly stated, this work throughout will implicitly refer to natural fractures.

2. Internal causes

2.1. Elastic deformation of wellbore walls

The theory behind radial expansion of thick-walled cylinder subjected to internal and external pressures can be traced back to the Lamé problem[14] (see Fig. 1).

If the internal and external pressures are referred to as p_a and p_b respectively, then the expression for the resulting normal stresses in radial and tangential directions become,[1]

$$\sigma_r = \frac{p_a a^2 - p_b b^2}{b^2 - a^2} - \frac{a^2 b^2 (p_a - p_b)}{b^2 - a^2}\frac{1}{r^2}$$
$$\sigma_\theta = \frac{p_a a^2 - p_b b^2}{b^2 - a^2} + \frac{a^2 b^2 (p_a - p_b)}{b^2 - a^2}\frac{1}{r^2} \quad (1)$$

[1] Solution by Lamé and Clapeiron, "Memoire sur l'equilibre interieur des corps solides homogenes" *Mem. Par divers savants*, Vol. 4, 1883.

Table 1
Volume increase in the total hydraulic system at pumps-off, after Aadnøy[12].

	12 ¼ in. hole	8 ½ in. hole
Flowrate [gal/min]	660.5	396
ΔV, mud [bbl]	1.4	1
ΔV, open hole [bbl]	0.0315	0.057
ΔV, casing [bbl]	0.044	0.113

The corresponding radial deformation u can be expressed as,

$$u = \frac{1-\nu}{E}\frac{p_a a^2 - p_b b^2}{b^2 - a^2} r + \frac{1+\nu}{E}\frac{a^2 b^2 (p_a - p_b)}{\left(b^2 - a^2\right) r} \tag{2}$$

where E, ν are the Young's modulus and Poisson's ratio, respectively. Radial expansion and contraction of tubular elements is generally referred to as *ballooning*, and this phenomenon has been studied extensively in the petroleum industry, particularly when dealing with transient pressure surge and swab calculations due to pipe movement.[15,16] Elastic deformation of the borehole walls was originally considered the main mechanism behind the drilling mud reversible loss, which was thus firstly addressed as *ballooning*. More specifically, during circulation, the Equivalent Mud Weight (EMW) equals the Equivalent Circulating Density (ECD). The ECD corresponds to the Equivalent Static Density (ESD) plus the additional contribution coming from the frictional pressure losses caused by drilling fluid flowing in the annulus. It follows that during circulation the wellbore pressure is higher and causes a certain radial expansion of the wellbore, whose volume consequently increases. The latter results in drilling fluid temporally stored in the extra volume that has been generated. When pumps are shut down, the wellbore pressure decreases and the wellbore walls return to the pre-circulation status, with resulting reduction of the wellbore volume. The latter produces an unexpected mud flow returned to the wellhead. It was James A. Gill who first brought to the attention how borehole ballooning alters drilling responses, and in support of his claims, many field observations were collected and analyzed.[2–4] However, there are major difficulties with this view, and specific reasons why it is not fruitful. The reader will have noticed that while loss and gain events have been addressed as *ballooning* in the first section, the term has since been avoided when describing wellbore/fractures interaction, and for the most parts will continue to be. There are two reasons for this: first, the definition ballooning tends to be vague and intuitive, and secondly, there is an almost unavoidable element of unscientific value judgment in the very concept when applied to anything other than wellbore volume or mud volume expansion/contraction. It was Ref. 11 that first conducted a study (both numerical and analytical), meant to compare the effect of borehole and casing deformation to mud expansion and contraction caused by compressibility effect. As a result, it was concluded that mud ballooning was by far the most significant contribution, whilst elastic deformation of borehole and casing accounted for only a very minor part. Two well designs were investigated and the same conclusion was drawn. Aadnøy[12] performed his own calculation on the same example wells, but his conclusions did not change. The volume increment due to the elastic rebound of casing and borehole amounted for only 5% and 14% for the two cases studied. The second case had an open hole of 8 ½", whereas the first was 12 ¼". For the former, a narrower annulus between borehole/drillpipe and casing/drillpipe caused higher frictional pressure losses and thus larger ballooning magnitude. Nonetheless, for the most severe case, the mud volume involved was only about 7 gallons, which is almost negligible if compared to the 30–100 bbl generally observed during ballooning/breathing events,[3,4] as shown in Table 1.

More recently, Helstrup et al.[5] presented their own computations regarding the absolute volumetric expansion of wellbores as a function of linearly increasing wellbore pressure (with depth) and *in-situ* stresses. According to Helstrup et al.[5], elastic deformation may be significant when dealing with soft formations, large borehole diameters and very deep wells. Indeed, those aspects combined can lead to higher than expected mud volume retained by the deformed wellbore. This is true particularly when drilling High Pressure, High Temperature (HPHT) wells. In these cases, high values of mud weight are generally used, and this may lead to appreciable wellbore deformations. This results in apparent mud losses, which could be misinterpreted as a consequence of wellbore failure or presence of fractures. However, their work shows how the significant radial expansion at a critical pressure may consume a significant amount mud barrels before actual formation breakout. Helstrup et al.[5] provided their own expression for the radial displacement, which included also the effects of the *in-situ* stresses and pore pressure ($\sigma'_H = \sigma_H - \xi p$, σ'_h; ξ is the Biot–Willis coefficient, from Ref. 17. Assuming plane strain conditions and using the superposition principle,

$$u = \frac{a}{E}\left\{p_w(1+\nu) - \left(1-\nu^2\right)\left[\left(\sigma'_H + \sigma'_h\right) + 2\left(\sigma'_H - \sigma'_h\right)\cos 2\theta\right]\right\} \tag{3}$$

The total volume of the deformed wellbore was then approximated by the one of an elliptical cone with its top removed. Major and minor radii of the deformed wellbore were written as a function of u as given in Eq. (3). It was concluded that for a soft formation (such as shale or high porosity chalk), the change in borehole volume due to elastic deformation was estimated to be even larger than one barrel (1.094 bbl).

2.1.1. Assessment

As obvious and favored as elastic deformations of wellbore walls are, they are among the weakest explanations of loss/gain events. The fundamental problem is that all wells routinely withstand pressure fluctuations without ballooning considerably. Since elastic deformations appear as normal aspects of any wellbore in all drilling environments, they could hardly be considered as major sources of losses/gains. Moreover, if they happen in a regular and recurrent manner, they, by themselves, cannot easily account for breathing, which is an occasional event. Thus, elastic deformation arguments present an incomplete causal chain; the basic assumption, rarely explicated, must be that the pressure fluctuation somehow exceeds the abilities of the system to absorb and recover from it. At this point some of the criticisms raised in regard to the elastic deformation argument become pertinent: if the assumption is correct, then the interesting factor is no longer the solid displacement mechanism, but the special conditions that made it happen.[5] Compelling evidences, especially coming from the works of Bjørkevoll et al.[11] and Aadnøy[12], showed how the fluid volume rebound caused by the elastic deformation of the wellbore walls cannot be even closely compared to the 30 to 100 bbl that is generally observed during ballooning/breathing events.[3,4] This is especially true if only the pressure fluctuations deriving from circulation cycles are accounted for. The difference between ECD and ESD, combined with the relatively high stiffness of formation, casing, and riser, leads to extremely modest mud volume rebounds.[12] Nonetheless, under the special circumstances described by Ref. 5, the elastic deformation can produce somewhat appreciable mudflow returns. This is particularly true when changes in the mud density, rather than wellbore pressure fluctuations during circulation cycles, are studied. Such a scenario could result in well unloading, for example, through adaptive drilling techniques such as managed-pressure drilling (MPD), in which a few barrels of mud-flow return may be registered.

On the light of what has been said, it can be concluded that other mechanisms should be investigated to rightly address the breathing phenomenon and increase the understanding of its physical characterization.

2.2. Fluid volume expansion and contraction

A variety of approaches can be found herein: thermal volumetric changes, compressibility, but the common underlying theme is the alteration in the drilling fluid density. This subject has a distinguished history in petroleum engineering research, including the drilling area, where "compositional material balance" models (and variations thereon) have enjoyed long currency (e.g. Refs. 18–20). Babu[21] compared some of the compositional models available in the literature, together with other empirical correlations, to estimate measured p-ρ-T data of twelve muds. He found that the empirical correlation proposed by Ref. 22, presented by Eq. (4), could describe better the p-ρ-T of the analyzed drilling fluids.

$$\rho_m = \rho_{m0} \exp\left[\alpha\,(p - p_0) - \beta\,(T - T_0) \pm \gamma\,(T - T_0)^2\right] \tag{4}$$

Where ρ_m is the mud density at the specified temperature T and pressure p, whilst $\rho_{m0}, \alpha, \beta, \gamma$ are empirical constants to be determined by means of linear regression of p-ρ-T measured data. The remaining T_0 and p_0 are the temperature (59 °F) and pressure (14.67 psi) at standard conditions, respectively. Based on Kutasov[22] correlation, Babu[21] developed an expression for the static pressure (in terms of ESD) which incorporates the p-ρ-T behavior of the mud, the surface T and p, the thermal gradient, and the well's depth D:

$$ESD = \frac{p - p_0}{0.052D} = \frac{1}{0.052\alpha D} \ln \frac{1}{1 - F\,(D)} \tag{5}$$

In Eq. (5), $F\,(D)$ is a function whose form depends on the sign of the $\gamma\,(T - T_0)^2$ term in Eq. (4). It shall be noted that negative sign of the term is for water-based muds and the positive sign for oil-based muds. More recently, Zamora et al.[23] measured the volumetric behavior of a wide range of oils, synthetics and brines, used as a base for many drilling fluids, under extreme temperatures and pressures. As a result, they could provide the values of the correlation coefficients in Eq. (6), for ranges of T and p exceeding those of previous publications.

$$\rho_i = \left(a_1 + a_2 p + a_3 p^2\right) + \left(b_1 + b_2 p + b_3 p^2\right) T \tag{6}$$

In Eq. (6), ρ_i is the density of the oil or brine under consideration and a_i, b_i the correlation coefficients. To demonstrate the validity of Eq. (6), Zamora et al.[23] implemented it in a compositional, material balance model used to predict the mud density as a function of temperature and pressure.

Regardless of the p-ρ-T model, to achieve an accurate estimation of the mud density, the temperature profiles during drilling must be determined first. Fig. 2 presents an example of temperature profile of a drilling mud being circulated down the pipe and through the annular space, versus depth. In this case, the drilling mud, entering to this section of the well, initially has a temperature lower than the formation. This results in a heat transfer from the formation to the drilling fluid. As a result of this heat exchange, the formation is cooled down at the deeper parts in the vicinity of the wellbore, heating up the drilling fluid in contact with it. Moving up the annulus, the heated mud causes an increase of temperature in the upper sections of the well, while also having a heat exchange with the fluid inside the pipe. Consequently, the whole heat exchange process leads to different temperature profiles inside the pipe and annulus (Fig. 2).

According to Ref. 24, the drillpipe acts as a counter-current heat exchanger, with mud temperature inside the pipe (or tubing)

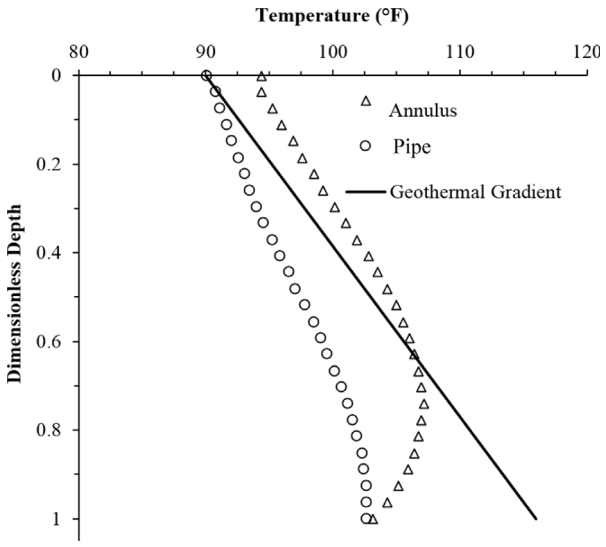

Fig. 2. Illustration of the various temperatures in the well (CFD solution after Foroushan[28])

T_t being lower than the mud temperature in the annulus T_a. To obtain the temperature profiles shown in Fig. 2, several implicit solutions have been proposed in the literature, including the ones of Corre et al.[25], Arnold[26], and Kabir et al.[27]

By performing extensive parametric studies, Karstad and Aadnoy[24] derived simple analytical solutions for the temperature behavior at different locations (namely mud return temperature at surface and bottom-hole temperature) for static and circulating conditions. For instance, the temperature after a finite circulation period has been expressed as:

$$T = T^0\,(1 - \delta) \tag{7}$$

The fundamental point of Eq. (7) is the application of the relative deviation of the temperature from its virgin value, denoted as δ. Accordingly, δ assumes different expressions depending on the location under consideration. At the bottom,

$$\delta_{bh} = \frac{c_1 f\,(t_D)}{1 + f\,(t_D)^{c_2}} \tag{8}$$

while at the return line we have,

$$\delta_{out} = 1 - \frac{1 + c_3 f\,(t_D)}{1 + f\,(t_D)^{c_4}} \tag{9}$$

In both Eq. (8) and (9), $f\,(t_D)$ represents a dimensionless temperature function, and the constants c_1, c_2, c_3, c_4 are calculated based on short and long time frames analysis.[24,27] Because the heat exchange process is strongly dependent on flowrate, each of the aforementioned constants were found to be approximated well by the following polynomial relation[24]:

$$c_i = k_1 + k_2 q + k_3 q^2 \tag{10}$$

The flow rate is expressed by q, and k_i are coefficients to be experimentally determined. In a subsequent publication, Karstad and Aadnoy[29] proposed their own analytical model for the p-ρ-T dependence of drilling fluids. Their model is based on the following expression:

$$\frac{d\rho_m}{dz}\,(p, T) = \frac{\partial \rho_m}{\partial p}\frac{dp}{dz} + \frac{\partial \rho_m}{\partial T}\frac{dT}{dz} \tag{11}$$

The assumption behind Eq. (11) is that both pressure and temperature are unique function of depth, z. Combining the studies of Peters et al.[19] regarding drilling fluids effective compressibility

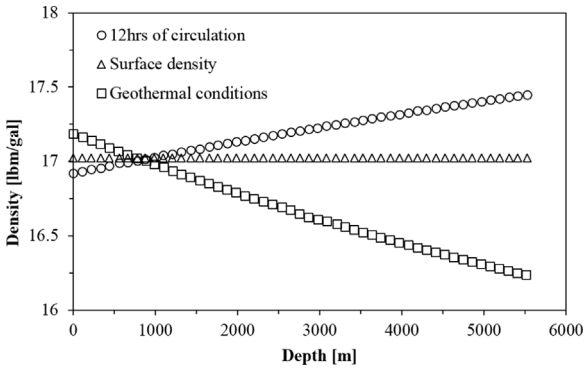

Fig. 3. Different density profiles after Karstad[6].

and extending the latter to the isobaric coefficient of thermal expansion, the following equation of state was derived.

$$\Gamma(p,T) = \gamma_p (p-p_0) + \gamma_{pp} (p-p_0)^2 + \gamma_T (T-T_0) + \gamma_{TT} (T-T_0)^2 + \gamma_{pT} (p-p_0)(T-T_0) \quad (12)$$

The values of γ_i are generally unknown and must be determined for the mud from density measurements at different temperatures and pressures. Combining their temperature and density models, Karstad[6] analyzed mud ballooning effects during drilling of HPHT wells. To describe the proposed coupling, they studied a case of an 8 1/2" hole, where a mud with properties from Peters et al.[19] is circulated for 12 h.

As expected, it turned out that temperature and pressure variations deeply affect the mud density, with consequent return mud volume variations, as shown in Fig. 3. From the figure it can be observed how the mud density increases as circulation proceeds. This is a result of the continuous cooling of the well caused by the drilling fluid circulation. On the other hand, if circulation is halted and enough time is given to reach thermodynamic equilibrium, the mud density decreases due to heat transfer from the formation. With mud temperature increasing, the density decreases with consequent volumetric rebound. Altogether, the virtual loss (related to density increment) and the following virtual gain was estimated to be around 32 bbl. In a previous study, Aadnøy[12] also showed how significantly the flow rate can influence the magnitude of thermal mud ballooning due to its considerable impact on the heat transferred. By means of a rather simpler temperature profile model, Babu[7] estimated the maximum pit volume gain after circulation, based on the p-ρ-T relation given in Eq. (5). Linearity was the major assumption in the temperature profile at both initial and final conditions. In his model, Babu[7] also provided an expression for the rate of volume gain:

$$\frac{v_t}{v_\infty} = 1 - C_4 f(t_D) \quad (13)$$

where v_t and v_∞ are the volume at any time t and the volume after thermal equilibrium, respectively. The constant C_4 is determined by satisfying the initial condition. Based on the briefly described model, Babu[7] simulated a 8 5/8" well, 17,500 ft deep, and with a circulation rate of 300 gal/min. The simulation was performed for six different muds whose properties were reported in Refs. 21, 22.

Table 2 summarizes the estimated maximum pit gain and relative decrease in ESD after circulation (muds 1 and 3 being water based and the rest oil-based).

In agreement with what observed by Karstad[6], an apparent mud gain is estimated concurrently with a decrease in the ESD. This is a consequence of the formation heating up the static mud, with resulting expansion of the latter. It can also be observed that for diesel-oil- and mineral-oil-based muds, the estimated maximum gains are almost twice that for water-based muds of identical densities. A similar conclusion can be also made by analyzing the differences between the volume gain rates. For the sake of pragmatism, Babu[7] introduced the "half gain period" to address the time lapsed (hr) after circulation that is required to regain half of the total expelled volume. Depending on the density of the mud, half gain periods range between 4 to 9 h.

Table 2
Estimated values after circulation.[7]

Mud no.	Maximum pit gain [bbl]	Decrease in static pressure [psi]
1	20.5	291
3	11.1	375
4	34.9	264
6	21.0	287
9	29.0	211
12	19.7	230

2.2.1. Assessment

By and large, the fluid expansion/contraction arguments are superior in one respect to the others considered up to this point. One of the strongest features of these models is the amount of mud rebound estimated. As shown in the previous section, the calculated drilling fluid volumes, apparently lost and gained, are mostly in the range of 20–45 bbl. Those estimations are in agreement with most of the field observations (e.g. Refs. 3, 4, 30, 31). Recognizing that an understanding of ballooning/breathing often depends on the characteristics of the drilling environment, the aforementioned authors postulated causal mechanisms – such as thermal dilatation and compressibility in HPHT wells – to explain why loss and gain events occur. This is a significant step. Yet, as intriguing as some of these explanations are, they seem as a lot to rely on certain assumptions, which the authors leave implicit, about the nature of breathing. If these assumptions are made explicit, they will leave enough causes for hesitation. What has not been stressed enough is why wellbore breathing represents such a concern for the drilling industry. The main hazard is related to the fact that misinterpretation of loss/gain events may jeopardize kick detection operations and lead to kick misdiagnosis. In other words, breathing and reservoir influxes have many similarities, including the *time frame*. Pit gain and flow increment are usually experienced in a time range that goes from minutes to few hours.[30–32] This unfortunately happens to be the time frame characterizing also reservoir fluid influxes, i.e. kicks.[32,33] The mudflow return time related to mud thermal ballooning is much longer than the pit gain time recorded during a kick (e.g. 10–12 h as shown by Refs. 6, 7).

In their industrial publication, Yuan et al.[32] provided a quite clear representation of the different pit gain signatures during flow check (Fig. 4). When circulation is halted and pumps shut down, the thermal expansion of the mud (red curve) shows a very slow rate of pit gain when compared with the faster pit gain rate of breathing and kick. Overall, thermal transients are much longer than pressure propagation. This causes pressure-related events to occur and stabilize faster than thermal-related ones. It follows that similarities in both magnitude and time frame complicate the differentiation of the two pressure-related influxes. Because of the time frame characterizing mud rebound caused by thermal dilatation, the models presented therein cannot provide the industry with the necessary answers. In other words, if wellbore ballooning/breathing is explained solely by thermal expansion/contraction arguments, no useful insights are given for real time ballooning/breathing discrimination. The latter is recognized to be a much needed know-how by the industry,[34–38] and that is why other physical mechanisms shall be explored.

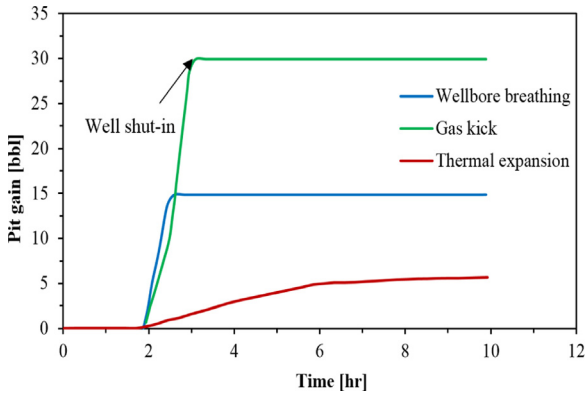

Fig. 4. Different pit gain signatures during flow check, after Yuan et al.[32]

3. External causes

Under this denomination are circumscribed all the causes of wellbore breathing related to the interaction of the well with something "external", namely the surrounding formation. Tare et al.[8] provided a comprehensive view on borehole breathing. Local geological characteristics related natural fractures, wellbore design and trajectory, and drilling operational conditions have been listed as the major players behind loss/gain events. Accordingly, breathing in Fractured Formations (FFs) is commonly observed under different circumstances (FFs refer to the presence of natural and/or drilling induced fractures). Among them: (1) drilling through zones characterized by a limited fracture network, with negligible leak off into the surrounding formation; (2) drilling in deep-water environments with a narrow operating window between pore pressure and fracture gradient; (3) drilling long wells with high inclination angles.[8,30,39] If, while circulating the drilling mud, the bottom-hole pressure increases over the fracture opening/initiation pressure, drilling fluid will migrate into hydraulically connected fractures intercepting the well (in this paper, the term initiation stands for the pressure necessary to start a fracture from the wellbore, whereas opening stands for the pressure to start the opening of an already existing fracture). As soon as circulation is stopped, the bottom-hole pressure decreases and may cause the fractures to close. This occurs during a pump-off period (connection, tripping or flow check operations) and may cause a sizable amount of mud to be returned back into the wellbore. Given the importance of understanding the mechanisms behind drilling fluid flow in fractures, the industry and many researches have made considerable efforts to model these phenomena. Dyke et al.[40] first showed how to distinguish between losses through a porous matrix and those in natural fractures. Lietard et al.[41] derived curves for mud propagation versus time for different hydraulic apertures, based on numerical solutions of the governing equations. Subsequently, Liétard et al.[42] refined this work, presenting mud-loss volume versus time type-curves for estimation of the fracture aperture via curve matching. Sanfillippo et al.[43] used the diffusivity equation to model flow into natural fractures, under a constant pressure difference. They assumed Newtonian muds and a non-deformable fracture, with a constant aperture. No fluid exchange with the porous matrix was allowed. Di Federico[44] studied the flow of a non-Newtonian fluid through a variable fracture aperture. An equivalent fracture aperture for three flow geometries have been derived, namely: (1) flow perpendicular to aperture variation; (2) flow parallel to aperture variation; (3) flow in an isotropic aperture field. The model developed by Ref. 45 makes use of the diffusivity equation and considers a constant aperture approximation. Non-Newtonian fluids have been considered. As output

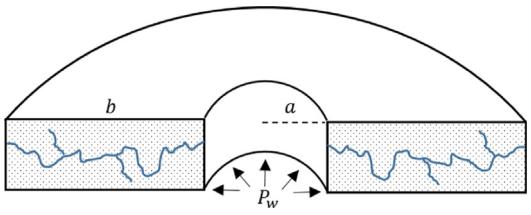

Fig. 5. Schematic cross sectional view of the open-hole intersecting a fracture network of finite length.

of the model, the fracture aperture values were calculated and compared with those measured by electric imaging logs. Lavrov and Tronvoll[46] developed a one-dimensional linear model of mud loss into a single fracture and performed a sensitivity analysis to study the effects of different parameters on mud losses. Their model assumed Newtonian fluids. The latter model was extended to mud loss events in radial coordinates[47], and non-Newtonian fluids. Moreover, a linearized fracture deformation law was applied. In a more recent work, Lavrov and Tronvoll[48] modeled the mud loss events using a Cartesian coordinates system, and investigated the effects of fracture dimensions. Majidi et al.[49] developed a mathematical model to study total mud losses as a function of the main fracture-controlling parameters (aperture, extension and compliance) and fluid rheological properties. More recently, Huang et al.[50] reviewed the work of Liétard et al.[42], and presented a more direct and straightforward method to infer the fractures hydraulic width, based on the solution of the cubic equation. Finally, Feng and Gray[51] developed a numerical model to estimate fluid loss into a growing, induced-fracture driven by dynamic circulation pressure during drilling. When the actual wellbore breathing mechanics is considered, the models available in the literature can be categorized into two groups: (1) single fracture models; (2) poroelastic continuum models.

3.1. Single fracture models

This perusal of wellbore breathing in fractured formations, in its various forms, brings us to its flowering in the early 21st century. Although the names of Lavrov and Tronvoll are most readily identifiable, there are a number of other theorists whose works merit attention. The works of Lavrov and Tronvoll[46,47,48] related to flow into a single fracture have been reviewed for so long and so thoroughly (e.g., Refs. 9, 52, 53), that little can be added that is really new. This will make the present description (compared with the overview just completed) mercifully short. It is nonetheless necessary to cover certain points to round out our critique study on single fracture models. In their work on fluid flow into a deformable fracture, Lavrov and Tronvoll[46,47,48] showed expectable evolution and change in their views. Yet, some basic premises and assumptions are present throughout the works, including their borehole breathing investigation.[9] Among them:

- Single fracture intersected by the well (fracture networks are not considered).
- Drilling fluid and formation fluid are assumed to have the same properties.
- Both fluids are considered incompressible.
- Horizontal fracture of circular shape.
- Impermeable fracture walls.
- Linear fracture deformation law.

A schematic view of such a system is given in Fig. 5.

The fundamental governing equation is given by Reynolds' equation in cylindrical coordinates,[54] which implies that the cubic law is valid for flow inside the fracture.

$$\frac{\partial h}{\partial t} - \frac{\partial}{\partial r}\left(\frac{h^3}{12\mu}\frac{\partial p}{\partial r}\right) - \frac{h^3}{12\mu}\frac{1}{r}\frac{\partial p}{\partial r} \tag{14}$$

Eq. (14) is valid for Newtonian fluids only, and the terms h, μ represent the fracture aperture and fluid dynamic viscosity respectively. If a non-Newtonian fluid with power law rheology is considered, the following expression, for the average fluid velocity in the fracture, can be derived[9]:

$$\overline{v} = -\frac{nh^{(n+1)/n}}{(2n+1)\,2^{(n+1)/n}K_{ci}^{1/n}}\left|\frac{\partial p}{\partial r}\right|^{n-1}\frac{\partial p}{\partial r} \tag{15}$$

In Eq. (15), n and K_{ci} represent the flow behavior index and consistency index, respectively. It follows that the cubic law ceases to hold in this case and the equation governing loss and gain is given by:

$$\frac{n}{(2n+1)\,2^{\frac{n+1}{n}}K_{ci}^{1/n}}\left[\frac{h^{\frac{2n+1}{n}}}{r}\frac{\partial p}{\partial r}\left|\frac{\partial p}{\partial r}\right|^{\frac{1-n}{n}} + \frac{\partial}{\partial r}\left(h^{\frac{2n+1}{n}}\frac{\partial p}{\partial r}\left|\frac{\partial p}{\partial r}\right|^{\frac{1-n}{n}}\right)\right] - \frac{\partial h}{\partial t} = 0 \tag{16}$$

Eq. (16) needs to be coupled with the linearized fracture deformation law:

$$h = h_0 + \frac{p}{K_n} \tag{17}$$

Where h_0, K_n are the initial fracture aperture and fracture's normal stiffness. The corresponding initial and boundary conditions are given as follows.[9]

$$\begin{aligned} &p = p_0 \quad @\,(a < r < b, 0)\\ &\frac{\partial p}{\partial r} = 0 \quad @\,(b, t > 0)\\ &p = p_0 + t\frac{(p_w - p_0)}{t_\varepsilon} \quad @\,(a, 0 < t < t_\varepsilon)\\ &p = p_w \quad @\,(a, t > t_\varepsilon) \end{aligned} \tag{18}$$

In Eq. (18), p_0 is the initial fracture pressure, p_w the wellbore pressure, and t_ε is a short time interval during which the pressure at the fracture mouth changes from p_0 to p_w. The non-linear partial differential equation (PDE) given by Eq. (16) was solved numerically by means of an explicit finite difference scheme. Based on the model outlined herein, wellbore breathing was simulated, and the effect of several parameters investigated. For instance, a mud loss/gain event was presented for the simple case of a Newtonian fluid. Both flow rates in and out, together with the cumulated lost volume are given in Figs. 6 and 7. The effects of rheological properties and fracture length, as some of the parameters that mostly affect wellbore breathing magnitude, were also investigated.

An important aspect governing the mechanical and transport characteristics of any fracture system is the roughness of fracture surfaces.[55] Based on the theoretical framework developed by Refs. 9, 46–48, 56 and Ozdemirtas et al.[57] conducted experimental tests and a numerical model study, investigating the impact of the fracture surface roughness on the cumulative volume of mud gain/loss during borehole breathing. In their numerical simulations, Ozdemirtas et al.[56] modeled a single 2D fracture with rough surfaces intersected by a wellbore (different intersecting location were also studied). To represent the rough surfaces of the fracture, the successive random addition and mid-point displacement methodology proposed by Ref. 58 was implemented.

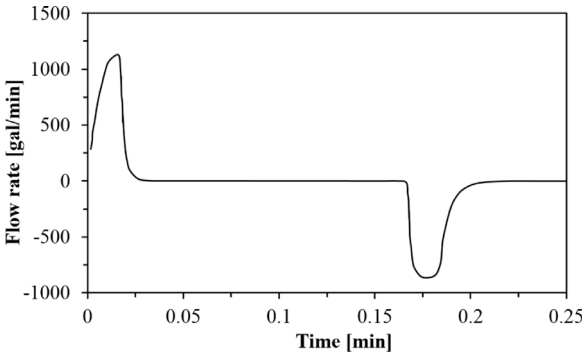

Fig. 6. Flow in and out of a 65 ft long fracture, intercepted by an 8 in. borehole. Initial fracture pressure and wellbore pressure were set to 2900 and 4350 psi respectively. Fracture stiffness and fluid dynamic viscosity are 2.2E06 psi/ft and 1 cP. After Lavrov and Tronvoll[9].

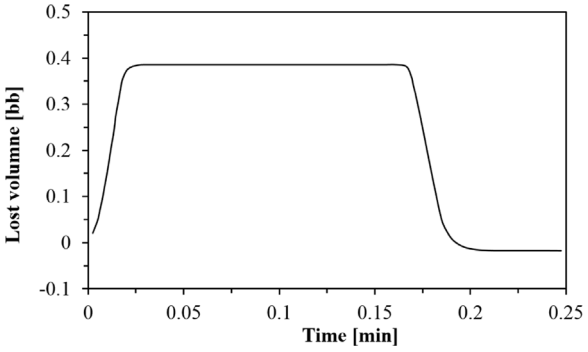

Fig. 7. Cumulative lost volume for the breathing case outlined in Fig. 6. After Lavrov and Tronvoll[9].

Two-dimensional fractal distributions were generated using fractional Brownian motion (FMB) for different grid sizes. If $B_H(x)$ is considered as a stationary stochastic process, its mean and variance can be expressed as:

$$\begin{aligned} &\langle B_H(x) - B_H(x_0)\rangle = 0\\ &\left\langle [B_H(x) - B_H(x_0)]^2 \right\rangle = |x|^{2H}\sigma_0^2 \end{aligned} \tag{19}$$

where x is any arbitrary point in space, whilst H is referred to as the Hurst exponent. The latter represents the degree of roughness of the FBM traces. The lower is H, the rougher is the distribution. It follows that $H = 1$ defines a perfectly smooth fracture. Altogether, the apertures resulting from the difference between two surfaces and surface roughnesses describe natural fracture surfaces of sedimentary rocks.[59,60] Based on their simulations, Ozdemirtas et al.[56] showed where the degree of roughness becomes critical in breathing events. In the example of Fig. 8, the average fracture aperture is set to be 0.04 in. for all the cases. It can be observed that rough fractures yield in general lower values of mud losses if compared to a smooth one. In addition, the effect of the random character of the width distribution (related to the standard deviation of the simulated data set) plays a significant role in breathing magnitude. In other words, it could be concluded that a set with a higher standard deviation of the fracture aperture (set D), would lead to a diminishing effect on borehole breathing in partially contacting fractures. Similar remarks were drawn for the mud gain case.

In a subsequent work, Ozdemirtas et al.[57] confirmed the observations of their simulations through a set of laboratory experiments, proving that fracture surface roughness and partially closing walls of the fissure lead towards a reduction of the mud gain and loss flow rates. Around the same period, Majidi et al.[61]

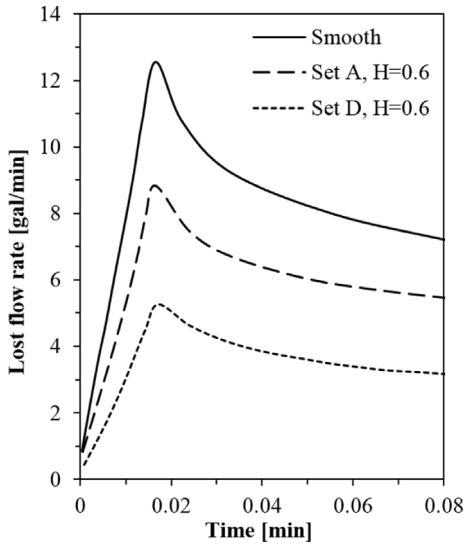

Fig. 8. Effect of fracture surface roughness degree on mud loss, after Ozdemirtas et al.[56]

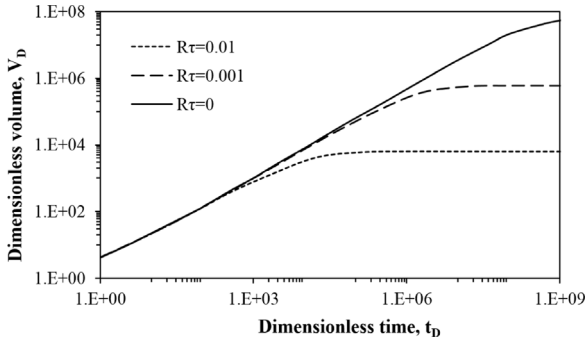

Fig. 9. Lost volume during wellbore breathing for different fluid yield stresses, after Majidi et al.[61]

extended the work of Lavrov and Tronvoll[9] to account for Yield-Power-Law (YPL) fluid rheology.

$$\tau = \tau_y + K_{ci}\dot{\gamma}^m \tag{20}$$

In Eq. (20), $\dot{\gamma}, \tau, \tau_y, m$ are the shear rate, shear stress, yield stress and YPL flow behavior index respectively. To generalize the outputs of their simulation, Majidi et al.[61] opted for a dimensionless representation of the governing equations, which were then solved by means of an implicit finite difference scheme. Results showed that both yield stress and shear thinning/thickening effects influence the dynamic of wellbore breathing.

In particular, it was observed that fluid losses in the fracture could be halted for significantly high values of yield stress (Fig. 9). The dimensionless parameter R_τ is a measure of the ratio between yield stress and applied overbalance pressure. It increases with increasing yield stress and was defined as:

$$R_\tau = \left(\frac{2m+1}{m+1}\right)\left(\frac{r_w}{h_0}\right)\frac{2\tau_y}{\Delta p} \tag{21}$$

When a zero value of fluid yield stress is considered, the fluid losses stops only because of the limited extension of the fracture. However, for increasing R_τ, the fluid flow halts altogether because the shear imposed is not large enough to overcome the yield stress resistance to motion. The model of Majidi et al.[61] applies the linearized fracture deformation law. The latter aspect

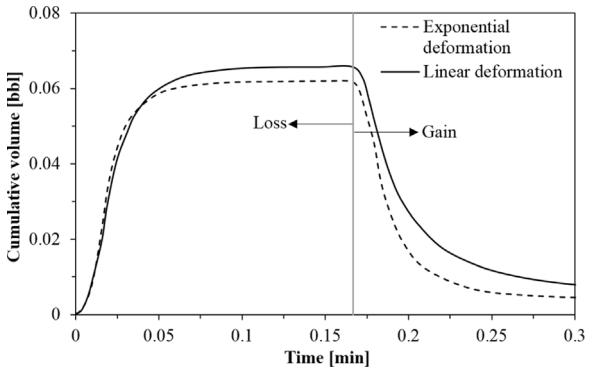

Fig. 10. Breathing for linear and exponential deformation laws, after Shahri et al.[62]

was then modified by Ref. 62 who considered the more realistic exponential deformation law.[63]

$$h = h^* \exp\left[\frac{-\vartheta\,(\sigma_n - p)}{3}\right] \tag{22}$$

In Eq. (22), h^* and ϑ represent the maximum fracture aperture preceding propagation and fracture compressibility, respectively. The normal stress is expressed by σ_n and is a function of the angle at which the fracture intercepts the wellbore, i, and in situ stresses.

$$\sigma_n = \sigma_v \cos^2 i + \sigma_h \sin^2 i \tag{23}$$

The horizontal stress σ_h is considered to be the minimum stress in the case of anisotropic in situ stress state, while σ_v is the in-situ vertical stress. Shahri et al.[62] compared the results of their simulation with the one obtained using the deformation law given in Eq. (17) (see Fig. 10).

It can be observed that the estimated breathing magnitude is larger in case of linearized deformation law, compared with the exponential one. According to Shahri et al.[62], the difference is believed to be related to the different pressure build up rates. In the exponential case, pressure builds up faster (due to larger resulting fracture aperture), leading to a faster exhaustion of the differential pressure that drives the loss/gain. A sensitivity analysis of this model was later performed by Ref. 64. In their work, the authors investigated the effect of several parameters on wellbore breathing. Among their conclusions, they argued that:

- Mud loss/gain severity increases with increasing fracture compressibility, β.
- For larger fracture length the cumulative losses increase.
- A larger wellbore radius leads towards a faster pressure buildup/drawdown of the fracture, especially at early times.
- Increasing values of normal stress σ_n bring about a reduction in the amount of cumulative losses.

Shahri and Mehrabi[65] extended the model of Majidi et al.[61] to a 2D fracture. As part of the work they also performed a sensitivity analysis, pointing out that the position of the borehole (with respect to the border of the 2D fracture) affects the mud flow dynamics. More specifically, faster mud loss rate decline was observed for wells intersecting the fracture at its center, rather than at the corners.

Finally, the work of Helstrup et al.[66] deserves a deeper discussion. The authors conducted a numerical analysis of borehole breathing occurring in a single natural fracture intersected by a wellbore using a time-dependent, poroelastic approach. The numerical study was performed by means of multi-physics capable finite elements method (FEM) package by ANSYS[67]. A two-dimensional plane-strain and isothermal model was chosen to

optimize the computation time. The single-phase flow assumption was kept, in analogy with the previous models, and fracture permeability was defined as:

$$k_{fr} = \frac{\mathrm{COD}^2}{12} \tag{24}$$

The acronym COD in Eq. (24) stands for crack opening displacement (namely, fracture aperture). In addition, the hydraulic and mechanical response of the fracture were coupled. The time-dependent pore pressure distribution in the rock matrix was obtained by solving the following 2D diffusivity equation.

$$\frac{\partial}{\partial x}\left(k_x \frac{\partial \Phi}{\partial x}\right) + \frac{\partial}{\partial y}\left(k_y \frac{\partial \Phi}{\partial y}\right) = -\left(Q - \lambda \frac{\partial \Phi}{\partial t}\right) \tag{25}$$

Where k_i is the matrix permeability, Φ the pore pressure, Q the source flow rate and $\lambda = \mu c_f \phi_m$, c_f and ϕ_m being the fluid compressibility and matrix porosity respectively. For a porous medium, the pore pressure can be regarded as a body force transmitted to the solid structure, and thus expressed as[68]:

$$b_j = -\frac{\partial \Phi}{\partial j} \tag{26}$$

The subscript j represents the space directional vector. Furthermore, if it is assumed that the boundary stresses and the distributed body forces acting on an element can be expressed by means of a unique linear stress–strain relationship, we can write[68]

$$q^e = \begin{Bmatrix} q_i^e \\ q_j^e \\ \vdots \end{Bmatrix} = K^e a^e + f^e$$
$$K^e = \int_{V^e}^{a} \mathbf{B}^T \cdot \mathbf{DB} \cdot \mathrm{dVol} \tag{27}$$
$$f^e = -\int_{V^e}^{a} \mathbf{N}^T b \mathrm{dVol} - \int_{V^e}^{a} \mathbf{B}^T \cdot \mathbf{D}\varepsilon_0 \mathrm{dVol} + \int_{V^e}^{a} \mathbf{B}^T \sigma_0 \mathrm{dVol}$$

The terms $q^e, a^e, \mathbf{N}, \mathbf{B}, \mathbf{D}$ represent the equivalent nodal force, nodal displacement, finite element shape function, strain matrix, and elasticity matrix, respectively. The solution is then found in terms of effective stresses,

$$\sigma_j' = \sigma_j - \alpha p = \mathbf{D}' \cdot (\varepsilon - \varepsilon_0) + \sigma_0' \tag{28}$$

In Eq. (28), ε and $\mathbf{D}'$ are the strain and the elasticity matrix containing the appropriate material properties. The subscript 0 denotes the reference in-situ values. The effect of a building-up mud cake (on the wellbore wall) was also included by expressing the time dependent permeability of the mud cake as[66]

$$k_{mc} = \frac{k_r - k_{mc}^{dyn}}{\exp^{\varphi t}} + k_{mc}^{dyn} \tag{29}$$

where k_{mc}^{dyn} is the dynamic mud cake permeability, and φ is a constant controlling the dependency of k_{mc} on the time lapse t. The possibility of fracture propagation was ultimately included in the study, by computing the equivalent mode I stress intensity factor at the fracture tip[69]

$$K_I^{eq} = \cos\frac{\theta_0}{2}\left(K_I \cos^2\frac{\theta_0}{2} - \frac{3}{2}K_{II}\sin^2\theta_0\right) \tag{30}$$

The classical intensity factors K_I, K_{II} refers to mode I (opening) and mode II (shear) respectively, whilst θ_0 defines the direction of fracture propagation, and it is given by the following expressions:

$$\theta_0 = 0, \text{ if } K_{II} = 0$$
$$\theta_0 = 2\tan^{-1}\left[\frac{K_I \pm \sqrt{K_I^2 + 8K_{II}^2}}{4K_{II}}\right], K_{II} \neq 0 \tag{31}$$

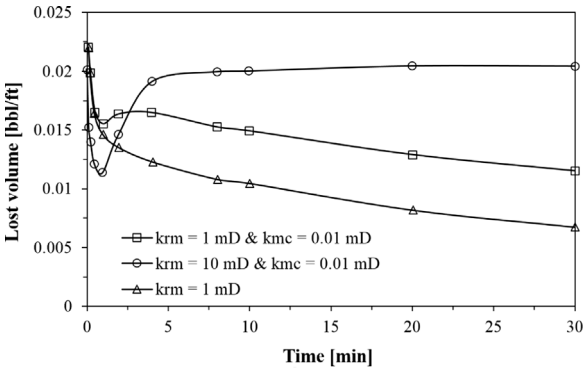

Fig. 11. Lost volume as a function of the matrix and mud cake permeability, after Helstrup et al.[66]

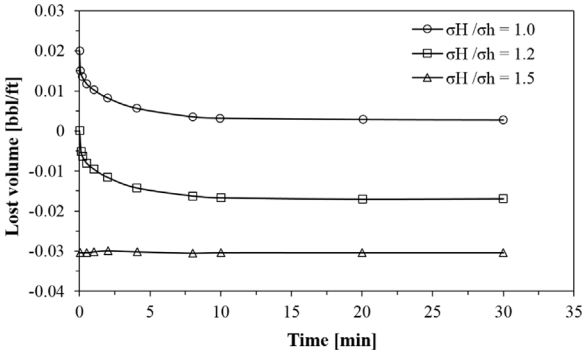

Fig. 12. Lost volume as a function of in-situ stress ratio, after Helstrup et al.[66]

Several simulations were conducted based on the model outlined herein. Among the outputs of Helstrup et al.[66] work, the effect of permeability and in-situ stress ratio is of particular interest. The total breathing volume was calculated considering both the wellbore deformation and fracture charging.

$$V_{bre} = 4\left(V_0 - V_{final}\right) \tag{32}$$

Fig. 11 shows a few examples of the simulations performed by letting matrix and mud cake permeability to vary. It was observed that breathing volume decreased with increasing filtration time and rock matrix permeability. When a mud cake is present, the breathing volume tends to increase until the mud cake permeability becomes constant (i.e. dynamic permeability). In general, the mud leak-off into the surrounding formation was found to be negligible for the tested rock matrix permeabilities.

Subsequently, the effect of in-situ stress contrast was investigated. For a natural fracture with orientation of 45° with respect to σ_H, Fig. 12 shows the effect of the stress contrast. With increase in the stress ratio, the breathing volume decreases. This is the result of two different factors[66]: (1) increase in the stress contrast contributes to reduce the intensity factor K_I at the fracture tip, thus stabilizing it; (2) the resulting normal component of the far field stresses is higher than the effective mud support or differential pressure (it is clear that for $\sigma_H/\sigma_h = 1.5$ the fracture is fully closed). The final consequence is a reduction in the combined ballooning/breathing volume of wellbore and fracture. In addition to the results, the effect of rock stiffness and fracture orientation have been investigated. It was concluded that for lower Young's modulus (softer formation), the ballooning/breathing volume significantly increases. Also, for fracture parallel to the maximum horizontal stress, mud losses tend to increase because of an increment in the fracture instability (higher K_I^{eq} at the tip).

3.1.1. Assessment

Single fracture models achieve one remarkable thing: they appeal to the spectrum of those who critique the thermal volumetric change models, and those one who find the elastic deformation explanation to be not appropriate to fully describe mud loss/gain events. In fact, the models just outlined can potentially provide the most reasonable method to describe wellbore breathing both in terms of magnitude and time frame. In the previous section throughout, it could be observed that cumulative mud losses occurring in a single fracture can effectively represent a portion of the total lost/gained volume exchanged through multiple fractures and/or fracture networks. The latter can be easily aligned to the mud rebound volumes generally observed in the field.[3,4] Furthermore, the time frame of this exchange is in line with the one expected for a pressure propagation process and thus like the time frame characterizing a reservoir influx (see Fig. 4). More specifically, the single fracture models can be quite effective for those cases where a single hydraulic fracture is present (if there are no natural fractures at preferred orientation for opening). In addition, in a naturally fractured system there may be only one fracture set (orientation) that opens and becomes hydraulically conductive, and in this case the single-fracture model is a way to simulate the mechanics of that orientation. However, when those scenarios do not apply, single fracture theories must at some point make the argument that considering a single fracture comes ultimately to violate one of the tenets of its existence: a naturally fractured formation (i.e. presence of a fracture networks), and/or several induced fractures. In this sense, an open-hole section of several hundred feet will most likely intercept more than just one or a few well-defined fractures.[70] One consequence is that single fracture models can be effective only if used as a base for discrete fracture network (DFN) representation of a fissured formation (i.e., Refs. 71, 72). DFN theorists, in particular, will have to acknowledge that any rational discretization, however complex, must make some provision for the fracture properties on which they rely, and that are required as inputs. Any suggestion that well defined properties for each modeled fracture is available *a priori* fails because of a characteristic – high degree of heterogeneity – that is intrinsic to the fractured formations (FFs) nature.[73,74] Moreover, the solution technique for the aforementioned single fracture models relies on numerical schemes. The latter require increasing computation time and power with increasing number of analyzed fractures and system complexity. Considering that wellbore breathing can complicate the already difficult practice of fingerprinting the changes in the return flow profile, hence undermining the reliability of kick detection, fast/real time computations are paramount and shall be preferred. Failure to resolve these matters when citing single fracture models as methods to describe borehole breathing, ultimately reduces the explanation to a dichotomous variable: if enough information and time are available, the method gives useful results, otherwise it does not. It needs hardly be pointed out that this dichotomy is not illuminating. Until some theory is developed concerning the optimization of system complexity vs. required inputs/computation time, we may confidently dismiss the single fracture argument as incomplete in its present stage.

3.2. Poroelastic continuum models

To date, only one wellbore breathing model can be inscribed into this category, and it was proposed by Baldino et al.[10]. Prior to this, Helstrup et al.[75] did consider poroelastic effects, but mostly focusing on the stability respone of the borehole and its subsequent interaction with a single natural fracture. On the other hand, the former authors considered FFs as overlapping continua of homogeneous pores (matrix) and homogeneous fracture networks (in analogy to what originally proposed by Refs. 76, 77). When Baldino et al.[10] modeled wellbore breathing, it appeared convenient to distinguish between two apparent fluid phases: one, mobile, occupying the fractures, and the other steady, occupying the pores. They proposed to consider an ad hoc zone defined as the hydraulically connected field (after zone diversification given by Ref. 78). The flow was assumed to occur in the fracture phase only, whereas the pore phase was regarded as the passive continuum. Interphase exchange was not allowed. For each point within these continua, phase properties are averaged over a carefully sized reference elementary volume (REV). Such a REV was assumed small enough to invalidate significant heterogeneity of the fractures involved in fluid transport. Hence, the vast majority of the fractures located in that domain will most likely be characterized by homogenized properties (spacing, aperture, orientation). The system ended up to dual-porosity/single-permeability. Interaction between the porous matrix and the network of fractures is limited to a poromechanical response only. Combining the appropriate equilibrium equations and the constitutive equations for this coupled poroelastic problem, the following governing equation were derived.[10]

$$\begin{aligned}(\lambda+2G)\frac{\partial}{\partial r}\left[\frac{1}{r}\frac{\partial}{\partial r}(ru)\right] &= \overline{\alpha}_1\frac{\partial p_1}{\partial r}+\overline{\alpha}_2\frac{\partial p_2}{\partial r}\\ \frac{k_1}{\mu}\frac{1}{r}\left[\frac{\partial}{\partial r}\left(r\frac{\partial p_1}{\partial r}\right)\right] &= \frac{\overline{\alpha}_1}{B_{u1}K_{u1}}\frac{\partial p_1}{\partial t}\\ &\quad+\overline{\alpha}_1\frac{\partial}{\partial t}\left[\frac{1}{r}\frac{\partial}{\partial r}(ru)\right]\\ \frac{\overline{\alpha}_2}{B_{u2}K_{u2}}\frac{\partial p_2}{\partial t}+\overline{\alpha}_2\frac{\partial}{\partial t}\left[\frac{1}{r}\frac{\partial}{\partial r}(ru)\right] &= 0\end{aligned} \tag{33}$$

Where λ and G are the Lamé parameters,[79] $B_{u1}, B_{u2}, K_{u1}, K_{u2}$ are the generalized Skempton coefficients and bulk moduli for the case of drained pores/undrained fractures and drained fractures/undrained pores, respectively.[80] Finally, $\overline{\alpha}_1$ and $\overline{\alpha}_2$ are referred to as generalized Biot–Willis coefficients. The subscript (or parenthetical superscript) "one" denotes the fractures, while "two" refers to the pores. In this sense, p_1 and p_2 are the fracture and matrix pore pressure, while k_1 is the fracture permeability. For naturally fractured formations, the latter was defined as a function of the fracture aperture after Jones Jr[81], and the exponential deformation law given in Eq. (22) was considered.

$$k_1 = \frac{h^3(\overline{x},t)}{12\varsigma} \tag{34}$$

In Eq. (34) ς represents the average fracture spacing. Eq. (33) was derived by means of the following assumptions:

- The fractures are initially empty, or otherwise saturated with fluid having the same properties as the wellbore fluid.
- Each continuum can be considered homogeneous and isotropic.
- Flow and elastic bulk deformations are in radial direction only.
- Flow into fractures is laminar and the fluid is considered Newtonian.
- Plane strain conditions apply.
- Wellbore is vertical and the problem is axially symmetric.
- No fracture propagation.

$$\begin{aligned}p_1(r,t) &= p_w+\pi\left(p_1^0-p_w\right)\\ &\quad\cdot\sum_{n=1}^{\xi_n}\frac{J_1(\xi_n b)J_0(\xi_n a)}{\left[J_0^2(\xi_n a)-J_1^2(\xi_n b)\right]}U(\xi_n r)\,e^{-C_{11}^*\xi_n^2 t}\end{aligned} \tag{35}$$

Table 3
Rock and system properties: (a) Rice and Cleary[83], (b) Cheng[84], (c) Elsworth and Bai[85].

Parameter	Berea Sandstone	Westerly Granite
K_2 [psi]	1.16×10^{6a}	3.6×10^{6a}
ν	0.20^a	0.25^a
b [ft]	12	12
α_2	0.78^b	0.45^b
K_f [psi]	2.9×10^5	2.9×10^5
h^*[in.]	1.5×10^{-2}	1.5×10^{-2}
B_2	0.551^b	0.810^b
ς	1	1
K_1 [psi]	1.125×10^{3c}	1.27×10^{4c}

Table 4
Vertical wellbore data.

Parameter	Value
Well depth [ft]	8200
ESD [lbm/gal]	10.0
ECD [lbm/gal]	10.35
r_w [in.]	8.5
H [ft]	328
p_1^0 [psi]	3530
σ_v gradient [psi/ft]	1
σ_h [psi]	4641

$$Q(t) = \frac{4\pi k_1 H}{\mu}\left(p_1^0 - p_w\right) \cdot \sum_{n=1}^{\xi_n} \frac{{J_1}^2(\xi_n b)}{J_0^2(\xi_n a) - J_1^2(\xi_n b)} e^{-C_{11}^* {\xi_n}^2 t} \tag{36}$$

$$V(t) = \frac{4\pi k_1 H}{\mu C_{11}^*}\left(p_1^0 - p_w\right) \cdot \left\{ \sum_{n=1}^{\xi_n} \frac{{J_1}^2(\xi_n b)}{\left[J_0^2(\xi_n a) - J_1^2(\xi_n b)\right]{\xi_n}^2} - \sum_{n=1}^{\xi_n} \frac{{J_1}^2(\xi_n b)\, e^{-C_{11}^* {\xi_n}^2 t}}{\left[J_0^2(\xi_n a) - J_1^2(\xi_n b)\right]{\xi_n}^2} \right\} \tag{37}$$

The fracture aperture has been assumed constant during an infinitesimal change in time and space for the purpose to derive the analytical solution. However, it was subsequently made time and space dependent when numerically computing Eqs. (35) to (37) by means of Eq. (22) (through the pressure distribution in the fracture) for finite time and space intervals. As shown in detail by Ref. 10, the analytical solution for the pressure distribution in the fractures, and thus the flow rate and related cumulative volume, could be obtained (Eqs. (35), (36), (37)). In Eqs. (35) to (37), J_ν and Y_ν are the Bessel functions of first and second kind respectively, of order ν,[82] with ξ_n being the positive roots of the transcendental equation

$$J_1(\xi_n b)\, Y_0(\xi_n a) - Y_1(\xi_n b)\, J_0(\xi_n a) = 0 \tag{38}$$

The coefficient C_{11}^* is the generalized consolidation coefficient and is given in Baldino et al.[10]. Based on the outlined solution, several results have been produced by analyzing two different rock formations: a compliant rock, Berea Sandstone, and a stiffer rock, Westerly Granite. Dual porosity media are not easy to characterize. Thus, to have the most accurate values of the formation properties, several references have been studied and Tables 3 and 4 summarize the data collected and the corresponding source of origin.

The horizontal state of stress is assumed isotropic and the fracture inclination is with respect to the vertical wellbore. To begin with, the mud loss case, while circulating, has been simulated for Berea Sandstone.

With reference to Fig. 13, some important observations can be made. Once the fluid has been compressed and the system

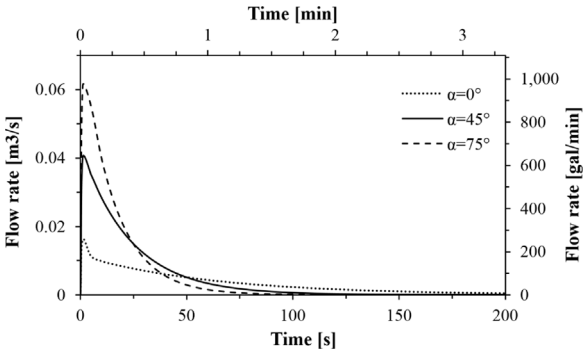

Fig. 13. Flow rate entering the fractures for different fracture inclinations. $\vartheta = 5.5 \times 10^{-4}\, psi^{-1}$, after Baldino et al.[10]

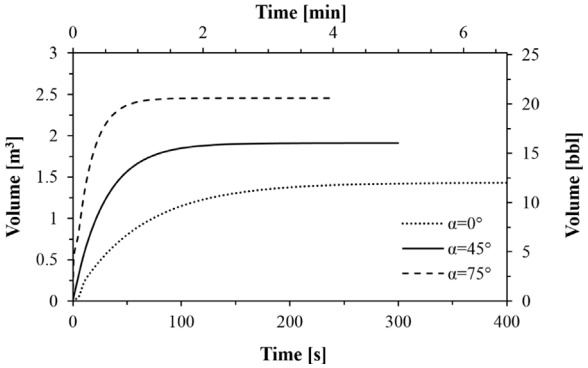

Fig. 14. Total volume lost in the fractures, for different fracture inclination angles and Berea Sandstone, after Baldino et al.[10]

deformed according to the imposed pressure inside the fractures, a decline is observed in the flow rate entering the fissures. Depending on the angle with whom the fracture intercepts the well, different flow curves are obtained. As expected, the lower the fracture inclination, the higher the resistance to fracture opening. The latter is caused by the more pronounced effect of the overburden on the stress normal to the fracture plane (see Eqs. (22) and (23)). If the normal stress is larger, the resulting fracture aperture will be smaller, as will the fractures effective permeability and porosity. Altogether this results in a smaller volume of fluid lost over a larger amount of time, as shown in Fig. 14.

For all three scenarios, the time frame is in line with that observed in the field.[31] It is noted that 12 to 21 barrels lost is also a realistic range, in the same order of magnitude for average mud losses registered while drilling breathing wells.[3,4,31] When a much stiffer formation was considered (i.e., Westerly Granite), it is expected to have significantly lower values of bulk elastic deformation, together with higher resistance to fracture aperture variation. This should lead towards a smaller amount of fluid stored in the fractures. This behavior was successfully represented by the proposed model and can be observed in Fig. 15. First, we notice the very short time needed to fill the fractures. After ten seconds there is almost no more flow in the fissured space. Moreover, the effect of fracture inclination is almost negligible.[48,86] This is because a less compliant fracture will resist further deformation, regardless of the normal stress acting on the fracture plane. Accordingly, the amount of lost volume is almost the same for the three cases considered, as shown in Fig. 16.

The effect of ECD was also investigated. If the ECD is increased, while everything else remains constant, this leads, as expected,

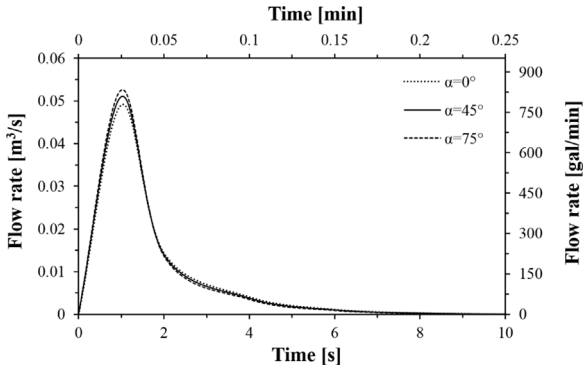

Fig. 15. Flow rate entering the fractures for different fracture inclinations. $\vartheta = 3.5 \times 10^{-5}\ psi^{-1}$, after Baldino et al.[10]

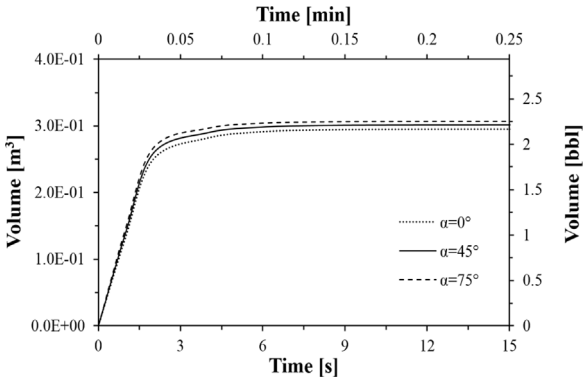

Fig. 16. Total lost volume, for different fracture inclination angles and Westerly Granite, after Baldino et al.[10]

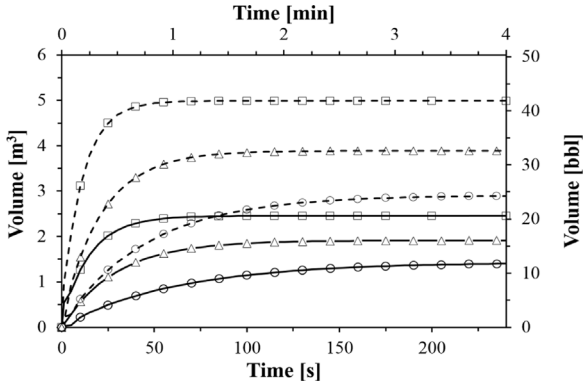

Fig. 17. The effect of ECD on wellbore breathing for different fracture inclinations (continuous lines represent ECD=10.35 lbm/gal, whilst dashed lines refer to ECD=12 lbm/gal), after Baldino et al.[10]

to a significant increment of the volume of mud that is lost into the fracture network, regardless of the fracture inclination. Higher ECD results in higher applied wellbore pressure (see Fig. 17). In turn, this causes larger fluid compression, higher elastic bulk deformations, and larger aperture variation. In their work the effect of fluid viscosity was also investigated and the shut-in drill pipe pressure (SIDPP) resulting from breathing was also modeled. It was shown how the proposed modeling of breathing could help with understanding the major differences between kicks and breathing, as shown in the SIDPPs comparison plot.

3.2.1. Assessment

There are many researchers and scientists who are not enamored of continuum models when describing fractured formations (i.e., Ref. 72). Yet even for such skeptics there are aspects to the structure and logic (if not the full content) of these models that makes them superior to those involving DFN representations. Among these aspects there are the following:

- No limitation on the number of fractures is posed.
- Analytical solutions provide with fast computations and do not require significant computation power.
- The number of input necessary to obtain quantitative and qualitative results is contained.

Because of the reasons mentioned above, the continuum model could give useful and realistic estimations of breathing events in fractured formations, both in terms of mud rebound volume and loss/gain time frame. The exponential decline of the lost/gained flow rate shown in Fig. 13, and generally described by Eq. (36), is in line with the observed exponential decline of the ECD during pumps-off, and caused by the mudflow returning to the wellbore.[30,87] Nonetheless, the continuum models have shortcomings, including the inability to fully represent the heterogeneity of a fractured formation. Moreover, the model proposed by Baldino et al.[10] revolves around significant assumptions. Among them, Newtonian fluid, absence of fractures propagation threshold and radial fluid flow urge a need of improvement over the present version. The authors have extended the breathing model to an inclined wellbore drilled in a FF, subjected to a non-hydrostatic state of stress.[38,88] An important aspect that all models are neglecting, including the latter, is the possibility to have multi-phase flow in the fractures. This is a very probable scenario when natural fractures are encountered and reservoir fluids, with different properties with respect to the drilling mud, are saturating the porous spaces. In conclusion, although the continuum models can potentially provide a significant enhancement over earlier models, it is still necessary to bestow a considerable effort to overcome their shortcomings.

4. Summarizing remarks

Wellbore ballooning/breathing is recurrent in drilling operations; it is global in its occurrence; and it affects the spectrum of drilling environments from simple onshore to deep-water offshore wells. Loss and gain events are a matter of considerable importance to every member of a rig crew, and seems to be of particular interest to many researchers today. Even though ballooning/breathing has been a little understood process, that is not for lack of trying. Reversible losses theorists have taken to heart the Maoist dictum to let a hundred schools of thought contend. While there is a nearly incomprehensible diversity of opinions regarding ballooning/breathing, these seem to boil down to a limited number of themes. These themes suffer from a number of logical failings, so that none by itself is adequate. Elastic deformation of the wellbore walls explanations seem worst in this regard, being virtually unable to account for the mud rebound volumes that are generally recorded in the field. Volumetric expansion and contraction of drilling fluid explanations are logically superior. They identify the characteristics of drilling environments that make them liable to wellbore ballooning, specify controlling mechanisms, and indicate causal chains between controlling mechanism and observed outcome. Yet existing explanations offer no general approach that would allow the understanding of ballooning /breathing from the time frame point of view (namely time required for the mud rebound volume to be returned to the surface). None of the aforementioned approach is necessarily incorrect. They are, as presently formulated, simply incomplete.

The only mechanism able to explain both rebound mud volumes and time frame is the one involving fluid invasion in opened or initiated fractures. Two major approaches to understanding the origin and mechanisms of wellbore breathing in fractured formations are the single fracture and continuum models. The former sees the wellbore intersecting a single fracture. The continuum theory suggests, in contrast, to consider fractured formations as overlapping continua of homogeneous pores (matrix) and homogeneous fracture networks. Complexity, in this view, is highly reduced. The continuum theory is better able to account for the presence of multiple fractures intersecting the open-hole, single fracture theory for the system heterogeneity. Both approaches have strong and weak points, and a synthesis of the two seems ultimately desirable. In this sense, the industry have successfully developed several methods and technology that enabled drilling through troublesome formation, where wellbore breathing would often increase NPT and related drilling costs, while lowering drilling efficiency.

CRediT authorship contribution statement

Silvio Baldino: Conceptualization, Methodology, Data curation, Original draft preparation, Writing, Literature review. **Meng Meng:** Writing - review & editing.

Declaration of competing interest

The authors declare that they have no known competing financial interests or personal relationships that could have appeared to influence the work reported in this paper.

Acknowledgments

The authors are thankful to the Tulsa University Drilling Research Projects member companies for their technical and financial supports.

Appendix. Industry approaches and remedies

The Bureau of Environmental Enforcement (BSEE) defines the loss of well control as an uncontrolled flow of reservoir fluid or other fluids. This means that mud flow return can and shall be treated with the same care as a reservoir influx. It is widely recognized that if a kick is correctly detected in its early stage, it can be managed more efficiently, with consequent reduction of the rig crew's stress level. The occurrence of wellbore breathing can greatly complicate kick detection operations, especially when checking the following common kick indicators[89]:

- Flow out measurements
- Pit volume gain measurements
- Gas cut in the bottom-up measurements

Cayeux and Daireaux[90] also developed a transient hydraulic model of the return flow to the mud pit, which proved able to detect gain and losses. However advanced, the model was not tested against borehole breathing. In addition, wellbore breathing is primarily encountered during connections. The latter is recognized to be the drilling mode where the vast majority (70%) of kicks are estimated to occur.[34] The correct interpretation of breathing versus kick is then paramount to enhance safety and increase drilling efficiency (avoid implementation of well control practices and thus reduce the non-productive time (NPT)). Moreover, if wellbore breathing is correctly identified, the most practical steps to contain it can be followed.[1]

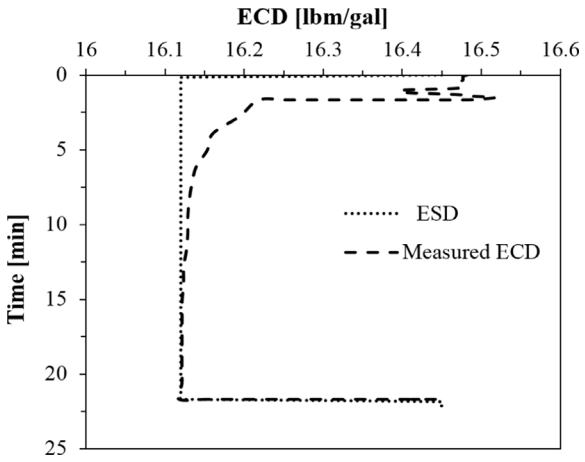

Fig. 18. Start of breathing in the 8 ½" section, ±45 bbl regained, after Ward and Clark[30].

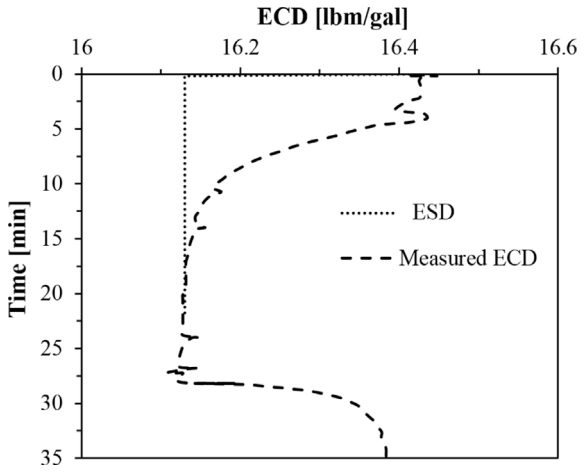

Fig. 19. Severe breathing in the 8 ½" section, ±85 bbl regained, after Ward and Clark[30].

A.1. Real time data monitoring

The accurate reading of real-time data can be very beneficial to successfully drill challenging wells. The downhole information that are gathered by Pressure While Drilling (PWD) and Logging While Drilling (LWD) tools can enable well-site personnel to implement corrective actions in the case of impending problems[91–95]. Roy and Power[96] reviewed several drilling events where PWD technology was successfully applied to avoid, identify, and respond to problematic scenarios, including kick detection, borehole washout and potential losses while running casing or liner. Among the other potential applications, Ward and Clark[30] have shown that the anatomy of borehole breathing can be efficiently detected by analyzing pressure while drilling data. In their work, the PWD tool can be used to diagnose whether the well is flowing or if borehole breathing is actually taking place. They argued that in case of mudflow return, the additional pressure losses resulting from circulation of the mud entering the wellbore, from the fractures, prevent ECD from falling rapidly to the static level.

On the other hand, mud losses will slow down the return to the ECD level observed prior the stop in circulation. From Figs. 18 and 19 it can be observed that the ECD exponentially declines to the ESD after pumps are shut down. As mentioned, this is caused by the extra frictional pressure losses resulting from circulation

of the mud entering the annulus from the fractures. Larger deviations from the squared profile (dotted line) indicate more severe breathing events, due to the larger mud rates involved (larger pressure losses in the annulus). This type of fingerprinting can be extremely beneficial to correctly diagnose wellbore breathing. However, the presence of dissolved gas in the mud may add a further complication to this type of readings. In fact, if reservoir fluids are dissolved in the mud, the final mud weight value after pumps-off may fall below the ESD. This is generally an indication of a potential kick.[34,97] Monitoring of real time data was also proposed by Ref. 98 to better assist the operators in detecting drilling issues. In their work, the authors presented two case studies where real-time time-lapse logging proved its value during drilling. Transmission and collection of the data was allowed by Advanced Composite Coil Tubing (ACCT) technology. The latter was connected to the bottomhole assembly (BHA). The middle section of the BHA is the one deputed to contain the measurement while drilling (MWD) sensors (i.e. pressure sub, resistivity tool, etc.). In the second case study, they illustrated how time-lapse logging can help to identify fractures in a shale formation. More specifically, the PWD was used to diagnose borehole breathing once the fractured zone had been intersected (in analogy to what done by Ref. 30). Although quite successful in diagnosing breathing, hundreds of formation-exposure hours were necessary (180) to identify the fractures through image logs and to characterize them in terms of dimension. Similarly, Bratton et al.[99] presented a method based on resistivity measurements used to detect the presence of fractures filled with a nonconductive fluid. Those resistivity readings were also used to correlate the different stages of fracture propagation and closure. Whilst not specific to loss/gain events, this method was applied to reveal the presence of fractures before breathing or losses have occurred, allowing preventive action to be deployed. Very recently, Golwalkar et al.[97] presented two case studies of two wells (NJ North-East 1 and Raag Deep Main-1) drilled in the same onshore block (RJ-ON-90/1, Rajasthan, India). Severe and recurrent wellbore breathing was observed in the first well. Nonetheless, the delayed identification of the event resulted in many unnecessary and counterproductive interventions (e.g., mud weight increase), with consequential high NPT and costs impact. The second well, drilled two months apart, was suffering from the same breathing issues. However, real time data monitoring, together with lessons learnt from the experience, were implemented, resulting in a smooth drilling operation and successful achievement of the planned objectives.

A.2. Managed pressure drilling (MPD)

MPD is an adaptive drilling technique whose scope is to enhance well control.[100,101] It usually employs a closed and pressurized drilling fluid system that facilitates precise control on the pressure profile along the wellbore. Mitigation of drilling hazards and optimization of drilling operation (NPT reduction) are the main benefits of efficient MPD deployment.[102] As mentioned, one of the advantages of managed pressure drilling technology is the presence of a closed and pressurized mud loop (Fig. 20).

The prerequisite for any closed system such as the one shown in Fig. 20 is the so-called rotary control device (RCD). The RCD is an essential device that diverts the flow away from the rig floor. It forms a friction seal around the drill pipe or kelly, and this is what creates a closed loop drilling system. The wellbore-pressure profile is then managed at the surface through the back-pressure pump (BPP) and the choke manifold. The acronym MPD was created recently,[103] and underbalanced drilling was its natural precursor. There are two categories of MPD[104]:

i. **Reactive**. One is prepared to deploy MPD as a contingency.

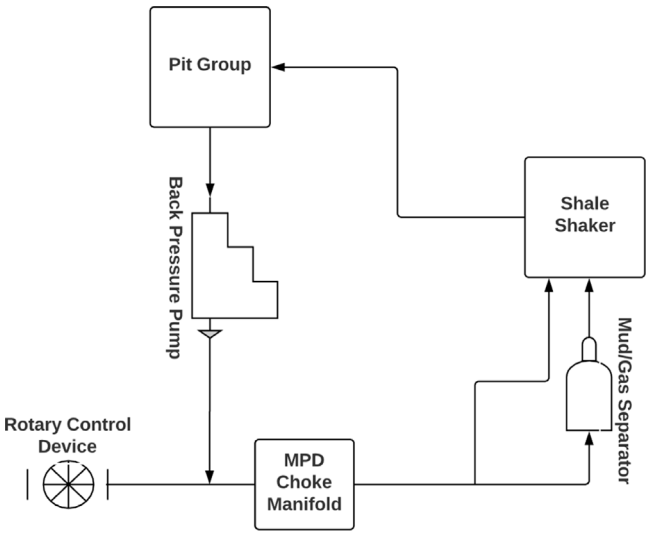

Fig. 20. Schematic diagram of a basic MPD closed system.

ii. **Proactive**. The drilling activities are planned ahead to take full advantage of MPD technology.

The proactive, or also called "walk the line" category is the one that offers the greatest benefits for both onshore and offshore drilling operations. The advantage of managed pressure drilling is that it adds another variable element to the terms contributing to the bottomhole pressure (BHP) or equivalent mud weight (EMW). The additional variable is the back pressure (BP) controlled by the BPP.

$$BHP_{MPD} = HH_{MW} + APF + BP \tag{39}$$

Where HH_{MW} is the hydrostatic head, governed by the mud weight, and APF the circulating annulus friction pressure. Based on the drilling hazard to which it has proved more effective, four key variations of MPD can be distinguished, and each of them takes advantage of the terms in Eq. (39) differently.

(1) **Returns flow control**. The only objective is to drill with a close mud loop for health, safety and environment compliance. Generally, for this type of variation, only the RCD is needed as additional component to the conventional drilling system.
(2) **Constant BHP (CBHP)**. This method aims to maintain a constant EMW (or bottomhole pressure) during both dynamic and static conditions (pumps on and off). The surface backpressure is managed to contribute to the HH in order to maintain the desired overbalance while circulation is stopped. This can be extremely beneficial when narrow margin between pore pressure and fracture gradient are encountered.
(3) **Dual Gradient Drilling**. The wellbore is subjected to two or more different pressure gradients along the annulus return path. This can be achieved by injecting lighter fluids or additives to the returning mud in specific locations (e.g., marine riser). Alternatively, an artificial lift from subsea pumps can be provided to generate a second gradient from that point to the surface.
(4) **Pressurized-Mudcap Drilling (PMCD)**. PMCD is generally implemented when severe or total losses are experienced. The methods involve the use of a pre-designed column of heavy fluid to be pumped to the backside through the RCD.[105] The mud cap that is thus created serves as an annulus barrier against returns to surface. The BP can be varied as an auxiliary contribution.

The advantages that MPD technology can bring are multiple,[104,106] and mitigation of wellbore ballooning/breathing is among them. Tirado Vargas et al.[107] presented a successful application of proactive MPD to drill under narrow mud weight window and severe wellbore breathing conditions. The drilled section was meant to pass through three different sands: (1) middle sand with low fracture gradient; (2) lower sand with higher pore pressure than fracture gradient. The well was located in the Burgos gas basin, north-western side of the Gulf of Mexico. Most of the offset wells did not reach the target zones (OV-20, OV-23, and OV-23 A), and that increased the drilling challenges due to higher geological uncertainty. Nonetheless, by proactive MPD implementation, the drillers were allowed to cross several sands without having any major well control events. The mud density and pump rates were designed ahead according to the sand being drilled, and backpressure was applied during static conditions (no circulation) to maintain a constant BHP (always higher than formation pressure). This CBHP variation of MPD significantly mitigated wellbore breathing events. In addition, the PMCD variation was used while tripping in order to avoid any returns from the formation associated with breathing effects. Mitigation of mud loss/gain events in the Cuervito Field (Burgos basin) was again achieved through managed pressure drilling, as explained by Ochoa Lugo et al.[108] The main producing zones of the Cuervito Field are sand with low permeability and abnormal pore pressure, and this translates into a very narrow mud weight window. In order to minimize the encountered problem and optimize drilling operations, an extensive study on 16 drilled wells was performed, including geological and geopressure information. As a result, MPD was chosen as the appropriate solution. The well Cuervito 17 was used as the pilot well for MPD application. The mud weight was reduced up to 6% of the originally planned value and backpressure was provided to compensate for this reduction and to maintain a constant BHP during static conditions. The final depth of the well was reached without major well control issues. Wellbore breathing was both mitigated and correctly identified. This also allowed for estimation of pore pressure and fracture gradient values. With the gathered experience, Cuervito 18, 19 and 20 were successfully drilled controlling breathing effects, reducing losses and saving NPT. Managed pressure drilling proved to be extremely effective in reducing the drilling challenges associated with ultra-high temperature wells (uHT). Loux et al.[109] reported the successful story of MPD application in two uHT appraisal wells (ATH-1 and ATH-2) drilled in the Arthit field, Gulf of Thailand. The reservoir targets were drilled with a 6 1/8" slim hole. The latter generates high ECD because of tight annular clearance and highly viscous mud rheological properties (used to ensure stability of drilling fluid when exposes to the extreme temperatures). If overbalanced drilling (high mud weight) is used, fracture gradient is easily exceeded, resulting in severe wellbore berthing. The CBHP variation was then implemented. The strategy involved the design of an underbalanced mud weight to prevent breathing, whilst MPD was used to maintain a constant BHP (above the pore pressure) by means of surface backpressure application. As a result, the operator was able to cut 50% of the costs and saved 20 days of drilling time. Further application of the MPD technology to mitigate wellbore breathing can be find in the industry publications of Refs. 110–113.

A.3. Liner drilling

Liner drilling (LD) technology has been proven quite successful to address such drilling issues as lost circulation, wellbore stability, depletion etc. (Ref. 114). The most relevant features of LD that make it a good candidate to mitigate the aforementioned drilling hazard can be summarized as follows.

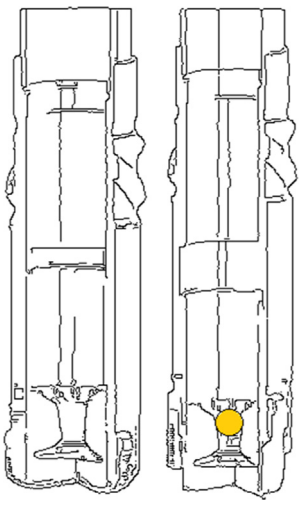

Fig. 21. CWD bit blade displacement; (left) before TD, (right) ball dropped at TD and blades displaced to the annulus. Modified after Rosenberg and Gala[119].

- Minimization of surge and swab due to minimal pipe tripping.
- Partial or total elimination of lost circulation problems because of smearing effect at borehole walls.[115]
- Better hole cleaning resulting from the close proximity between casing and borehole walls, leading to high annular velocity.

The smearing effect proved to be the most effective while drilling through fractured formations. In that case, the smeared cuttings could help in bridging the fractures because they are plastered against the wellbore walls.[116] An example of LD application to isolate an unstable formation was presented by Terrazas Romero et al.[117]. While drilling through the El Abra fractured formation (Gulf of Mexico), a 9 5/8" liner was drilled and set successfully without losses. In another Gulf of Mexico operation, Rosenberg et al.[118] showed how a 5 ½" liner could be drilled and set preventing losses and enabling trouble-free production tubing completion. More recently, Rosenberg and Gala[114] presented five case histories, in both shelf and deepwater Gulf of Mexico, where the application of LD technology allowed significant mitigation of several drilling hazards, including lost circulation and wellbore stability. The core parts of an LD system are the casing while drilling (CWD) drill bit and the liner hanger system (LHS). The CWD bit performs as a classical PDC bit until the total depth (TD) is reached. At that time, a ball is dropped through the liner running string into the bit, thereby plugging the nozzles.

The resulting pressurization of the casing string causes displacement of the steel blades PDC-cutting structure into the open-hole section (Fig. 21). Circulation is re-established through the cementing ports. The LHS is sketched in Fig. 22. The packing element is generally designed to prevent swabbing and premature setting, whilst keeping the cuttings away from the packing element as they pass by while being circulated. As mentioned, one of the advantages of LD technology is to mitigate lost circulation events. Based on this feature, Rosenberg and Gala[119] presented a case study where LD was successfully deployed to mitigate wellbore breathing. While drilling a 8 ½" sidetrack hole in the Gulf of Mexico shelf, severe borehole breathing was encountered, preventing the well from being drilled to its objective depth. After thorough analysis of the situation, LD was chosen as the most practical and cost-effective solution. The 8 ½" directional BHA was removed and a 7" CWD bit liner (with running tool, liner top packer and PBR) was lowered in the

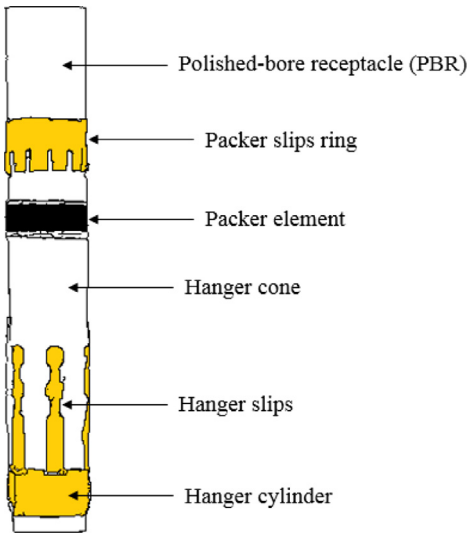

Fig. 22. Liner hanger system, modified after Rosenberg and Gala[119].

wellbore. After a few assessments during which losses and gains were recorded, the LD operation met the objective to combat the borehole breathing problems (where conventional drilling failed). Although the planned TD could not be reached, the CWD bit drilled to a satisfactory depth, enabling completion.

References

1. Power D, Ivan CD, Brooks SW. The top 10 lost circulation concerns in deepwater drilling. In: *SPE Latin American and Caribbean Petroleum Engineering Conference*. Society of Petroleum Engineers; 2003 January.
2. Gill JA. Charged shales: self-induced pore pressures. In: *SPE/IADC Drilling Conference*. Society of Petroleum Engineers; 1986 January.
3. Gill JA. Well logs reveal true pressures where drilling responses fail. *Oil Gas J (United States)*. 1987;85(11).
4. Gill JA. How borehole ballooning alters drilling responses. *Oil Gas J (United States)*. 1989;87(11).
5. Helstrup OA, Rahman MK, Hossain MM, Rahman SS. A practical method for evaluating effects of fracture charging and/or ballooning when drilling high pressure, high temperature (HPHT) wells. In: *SPE/IADC Drilling Conference*. Society of Petroleum Engineers; 2001.
6. Karstad E. Analysis of ballooning effects during drilling of high pressure high temperature wells. In: *European Petroleum Conference*. Society of Petroleum Engineers; 1998.
7. Babu DR. Effect of P–ρ–T behavior of muds on loss/gain during high-temperature deep-well drilling. *J Petrol Sci Eng*. 1998;20(1–2):49–62.
8. Tare UA, Whitfill DL, Mody FK. Drilling fluid losses and gains: case histories and practical solutions. In: *SPE Annual Technical Conference and Exhibition*. Society of Petroleum Engineers; 2001.
9. Lavrov A, Tronvoll J. Mechanics of borehole ballooning in naturally-fractured formations. In: *SPE Middle East Oil and Gas Show and Conference*. Society of Petroleum Engineers; 2005 January.
10. Baldino S, Miska SZ, Ozbayoglu E. A novel approach to borehole breathing investigation in naturally fractured formations. *SPE Drill Complet*. 2018.
11. Bjørkevoll KS, Vefring EH, Rommetveit R, Aadnøy B. Changes in active volume due to variations in pressure and temperature in HPHT wells. In: *7th Northern European Drilling Conference, Kristiansand*; 1994 October 4-6.
12. Aadnøy BS. *Modern Well Design*. 1st ed. New York City: CRS Press; 1996 Appendix B.
13. Maury V, Idelovici JL. February. Safe drilling of HP/HT wells, the role of the thermal regime in loss and gain phenomenon. In: *SPE/IADC Drilling Conference*. Society of Petroleum Engineers; 1995.
14. Timoshenko S, Goodier JN. *Theory of Elasticity*. 412, 1951:108, New York.
15. Lubinski A, Hsu FH, Nolte KG. Transient pressure surges due to pipe movement in an oil well. *Rev Inst Français du Pétrole*. 1977;32(3):307–348.
16. Mitchell RF. Dynamic surge/swab pressure predictions. *SPE Drill Eng*. 1988;3(03):325–333.
17. Biot MA, Willis DG. The elastic coeff cients of the theory of consolidation. *J Appl Mech*. 1957;15:594–601.
18. Hoberock LL, Thomas DC, Nickens HV. 'Bottom-hole mud pressure variations due to compressibility and temperature effects. In: *the 1982 IADC Drilling Technology Conference, Houston, March 9-11*; 1982.
19. Peters EJ, Chenevert ME, Zhang C. A model for predicting the density of oil-base muds at high pressures and temperatures. *SPE Drill Eng*. 1990;5(02):141–148.
20. Sorelle RR, Jardiolin RA, Buckley P, Barrios JR. Mathematical field model predicts downhole density changes in static drilling fluids. In: *SPE Annual Technical Conference and Exhibition*. Society of Petroleum Engineers; 1982 January.
21. Babu DR. Effects of PpT behaviour of muds on static pressures during deep well drilling-part 2: Static pressures. *SPE Drill Complet*. 1996;11(02):91–97.
22. Kutasov IM. Empirical correlation determines downhole mud density. *Oil Gas J*.. 1988;86(52):61–63.
23. Zamora M, Roy S, Slater KS, Troncoso JC. Study on the volumetric behavior of base oils, brines, and drilling fluids under extreme temperatures and pressures. *SPE Drill Complet*. 2013;28(03):278–288.
24. Karstad E, Aadnoy BS. Analysis of temperature measurements during drilling. In: *SPE Annual Technical Conference and Exhibition*. Society of Petroleum Engineers; 1997 January.
25. Corre B, Eymard R, Guenot A. Numerical computation of temperature distribution in a wellbore while drilling. In: *SPE Annual Technical Conference and Exhibition*. Society of Petroleum Engineers; 1984 January.
26. Arnold FC. Temperature variation in a circulating wellbore fluid. *J Energy Res Technol*. 1990;112(2):79–83.
27. Kabir CS, Hasan AR, Kouba GE, Ameen M. Determining circulating fluid temperature in drilling, workover, and well control operations. *SPE Drill Complet*. 1996;11(02):74–79.
28. Foroushan HK. Displacement of fluids in annuli. [Ph.D. thesis]. University of Tulsa; 2018.
29. Karstad E, Aadnoy BS. Density behavior of drilling fluids during high pressure high temperature drilling operations. In: *IADC/SPE Asia Pacific Drilling Technology*. Society of Petroleum Engineers; 1998 January.
30. Ward C, Clark R. Anatomy of a ballooning borehole using PWD tool. In *Workshop Overpressures in Petroleum Exploration, Pau, France*, 1998, April 7-8.
31. Ashley PR. Well control of an influx from a fracture breathing formation. In: *IADC/SPE Asia Pacific Drilling Technology*. Society of Petroleum Engineers; 2000 January.
32. Yuan Z, Morrell D, Mayans AG, Adariani YH, Bogan M. Differentiate drilling fluid thermal expansion, wellbore ballooning and real kick during flow check with an innovative combination of transient simulation and pumps off annular pressure while drilling. In: *IADC/SPE Drilling Conference and Exhibition*. Society of Petroleum Engineers; 2016.
33. Ridley KM, Jurgens M, Billa RJ, Mota JF. Eagle ford shale well control: Drilling and tripping in unconventional oil and gas plays. In: *SPE Unconventional Gas Conference*. Society of Petroleum Engineers.; 2013 January 28.
34. Fraser D, Lindley R, Moore D, Vander Staak M. Early kick detection methods and technologies. In: *SPE Annual Technical Conference and Exhibition, ATCE*. Society of Petroleum Engineers; 2014.
35. Johnson A, Leuchtenberg C, Petrie S, Cunningham D. Advancing deepwater kick detection. In: *IADC/SPE Drilling Conference and Exhibition*. Society of Petroleum Engineers; 2014 March..
36. Nayeem AA, Venkatesan R, Khan F. Monitoring of down-hole parameters for early kick detection. *J Loss Prev Process Ind*. 2016;40:43–54.
37. Tarr BA, Ladendorf DW, Sanchez D, Milner GM. Next-generation kick detection during connections: Influx detection at pumps stop (IDAPS) software. *SPE Drill Complet*. 2016;31(04):250–260.
38. Baldino S, Miska SZ, Ozbayoglu EM, Zhang J. Borehole-breathing/kick discriminator: Diagnostic tool and potential resource for in-situ formation characterization. *SPE Drill Complet*. 2019;34(03):248–267.
39. Erivwo OE, Adeleye OA. Narrow margin drilling in deepwater: Solution concepts. In: *SPE Deepwater Drilling and Completions Conference*. Society of Petroleum Engineers; 2012 January.
40. Dyke CG, Wu B, Milton-Tayler D. Advances in characterizing natural fracture permeability from mud log data. *SPE Form Evaluat*. 1995;10(03):160–166.
41. Lietard O, Unwin T, Guillot D, Hodder M. Fracture width LWD and drilling mud/LCM selection guidelines in naturally fractured reservoirs. In: *European Petroleum Conference*. Society of Petroleum Engineers; 1996 January.
42. Liétard O, Unwin T, Guillot DJ, Hodder MH. Fracture width logging while drilling and drilling mud/loss-circulation-material selection guidelines in naturally fractured reservoirs (includes associated papers 75283, 75284, 81590 and 81591). *SPE Drill Complet*. 1999;14(03):168–177.
43. Sanfillippo F, Brignoli M, Santarelli FJ, Bezzola C. Characterization of conductive fractures while drilling. In: *SPE European Formation Damage Conference*. Society of Petroleum Engineers; 1997.
44. Di Federico V. Non-Newtonian flow in a variable aperture fracture. *Transp Porous Media*. 1998;30(1):75–86.

45. Verga FM, Carugo C, Chelini V, Maglione R, De Bacco G. Detection and characterization of fractures in naturally fractured reservoirs. In: *SPE Annual Technical Conference and Exhibition*. Society of Petroleum Engineers; 2000 January.
46. Lavrov A, Tronvoll J. Mud loss into a single fracture during drilling of petroleum wells: Modeling approach. In: *Development and Application of Discontinuous Modelling for Rock Engineering: Proceedings of the 6th International Conference ICADD-6, Trondheim, Norway*, 2003 October 5–8; 189-198.
47. Lavrov A, Tronvoll J. Modeling mud loss in fractured formations. In: *Abu Dhabi International Conference and Exhibition*. Society of Petroleum Engineers; 2004 January.
48. Lavrov A, Tronvoll J. Numerical analysis of radial flow in a natural fracture: applications in drilling performance and reservoir characterization. In: *Abu Dhabi International Petroleum Exhibition and Conference*. Society of Petroleum Engineers; 2006 January.
49. Majidi R, Miska S, Thompson LG, Yu M, Zhang J. Quantitative analysis of mud losses in naturally fractured reservoirs: the effect of rheology. *SPE Drill Complet*. 2010;25(04):509–517.
50. Huang J, Griffiths DV, Wong SW. Characterizing natural-fracture permeability from mud-loss data. *SPE J*. 2011;16(01):111–114.
51. Feng Y, Gray KE. Modeling lost circulation through drilling-induced fractures. *SPE J*. 2017.
52. Ozdemirtas M. Numerical and experimental investigations of borehole ballooning in smooth and rough fractures. [Master of Science Thesis]. University of Alberta; 2009.
53. Shahri MP, Zeyghami M, Majidi R. Investigation of fracture ballooning and breathing in naturally fractured reservoirs: effect of fracture deformation law. In: *Nigeria Annual International Conference and Exhibition*. Society of Petroleum Engineers; 2011 January.
54. Zimmerman RW, Bodvarsson GS. Hydraulic conductivity of rock fractures. *Transp Porous Media*. 1996;23(1):1–30.
55. Babadagli T, Develi K. On the application of methods used to calculate the fractal dimension of fracture surfaces. *Fractals*. 2001;9(01):105–128.
56. Ozdemirtas M, Babadagli T, Kuru E. Numerical modelling of borehole ballooning/breathing-effect of fracture roughness. In: *Canadian International Petroleum Conference*. Petroleum Society of Canada; 2007.
57. Ozdemirtas M, Babadagli T, Kuru E. Experimental and numerical investigations of borehole ballooning in rough fractures. *SPE Drill Complet*. 2009;24(02):256–265.
58. Voss RF. Random fractal forgeries. In: *Fundamental Algorithms for Computer Graphics*. Berlin, Heidelberg: Springer; 1985:805–835.
59. Develi K, Babadagli T. Quantification of natural fracture surfaces using fractal geometry. *Math Geol*. 1998;30(8):971–998.
60. Babadagli T, Develi K. Fractal characteristics of rocks fractured under tension. *Theoret Appl Fracture Mech*. 2003;39(1):73–88.
61. Majidi R, Miska SZ, Yu M, Thompson LG. Fracture ballooning in naturally fractured formations: mechanism and controlling factors. In: *SPE Annual Technical Conference and Exhibition*. Society of Petroleum Engineers; 2008 January.
62. Shahri MP, Zeyghami M, Majidi R. Investigation of fracture ballooning-breathing using an exponential deformation law and herschel- bulkley fluid model. *Spec Top Rev Porous Media*. 2012;3(4).
63. Bruel D, Cacas MC, Ledoux E, De Marsily G. Modelling storage behaviour in a fractured rock mass. *J Hydrol*. 1994;162(3–4):267–278.
64. Mehrabi M, Zeyghami M, Shahri MP. Modeling of fracture ballooning in naturally fractured reservoirs: A sensitivity analysis. In: *Nigeria Annual International Conference and Exhibition*. Society of Petroleum Engineers; 2012 January.
65. Shahri MP, Mehrabi M. A new approach in modeling of fracture ballooning in naturally fractured reservoirs. In: *SPE Kuwait International Petroleum Conference and Exhibition*. Society of Petroleum Engineers; 2012 December.
66. Helstrup OA, Chen Z, Rahman SS. Time-dependent wellbore instability and ballooning in naturally fractured formations. *J Petrol Sci Eng*. 2004;43(1–2):113–128.
67. ANSYS. *Theory Reference. V6. 1*. 2002 Chap. 6.
68. Zienkiewicz OC, Taylor RL. The finite element method. In: *The Basics, vol. 1*. 5th ed. Melbourne: Butterworth; 2000 Chaps. 2 and 7.
69. Rahman MK, Hossain MM, Rahman SS. An analytical method for mixed-mode propagation of pressurized fractures in remotely compressed rocks. *Int J Fract*. 2000;103(3):243–258.
70. Wang H, Chen M, Wei S, Lu Y, Nie Z, Liang Q. Breathing effect of sandstone reservoir formed in barrier coastal sedimentary system. In: *ISRM International Symposium-EUROCK 2020*. International Society for Rock Mechanics and Rock Engineering; 2020 November.
71. Biryukov D, Kuchuk FJ. Transient pressure behavior of reservoirs with discrete conductive faults and fractures. *Transp Porous Media*. 2012;95(1):239–268.
72. Kuchuk F, Biryukov D, Fitzpatrick T. Fractured-reservoir modeling and interpretation. *SPE J*. 2015;20(05). 983-1.
73. Belfield WC, Sovich JP. Fracture statistics from horizontal wellbores. *J Can Pet Technol*. 1995;34(06).
74. Bour O, Davy P. Connectivity of random fault networks following a power law fault length distribution. *Water Resour Res*. 1997;33(7):1567–1583.
75. Helstrup OA, Rahman K, Chen Z, Rahman S. Poroelastic effects on borehole ballooning in naturally fractured formations. In: *SPE/IADC Drilling Conference*. Society of Petroleum Engineers; 2003.
76. Barenblatt GI, Zheltov YP. Fundamental equations of filtration of homogeneous liquids in fissured rocks. In: *Soviet Physics Doklady (Vol. 5)*. 1960:522, November.
77. Warren JE, Root PJ. The behavior of naturally fractured reservoirs. *SPE J*. 1963;3(03):245–255.
78. Bear J, Tsang CF, De Marsily G. *Flow and Contaminant Transport in Fractured Rock*. De Marsily, G Academic Press; 2012.
79. Sadd MH. *Elasticity: Theory, Applications, and Numerics*. Academic Press; 2009.
80. Berryman JG, Wang HF. The elastic coefficients of double-porosity models for fluid transport in jointed rock. *J Geophys Res: Solid Earth*. 1995;100(B12):24611–24627.
81. Jones Jr FO. A laboratory study of the effects of confining pressure on fracture flow and storage capacity in carbonate rocks. *J Pet Technol*. 1975;27(01):21–27.3.
82. Watson GN. *A Treatise on the Theory of Bessel Functions*. Cambridge university press; 1922.
83. Rice JR, Cleary MP. Some basic stress diffusion solutions for fluid-saturated elastic porous media with compressible constituents. *Rev Geophys*. 1976;14(2):227–241.
84. Cheng AH-D. *Poroelasticity (Theory and Applications of Transport in Porous Media, vol. 27)*. Cham, Switzerland: Springer International Publishing; 2016.
85. Elsworth D, Bai M. Flow-deformation response of dual-porosity media. *J Geotech Eng*. 1992;118(1):107–124.
86. Gao R, Li J, Liu G, Yang H, Luo K, Zhai W, Zhang X, Zhang R. Experimental study on typical characteristics of borehole breathing under different pressure and rock type conditions. *J Natural Gas Sci Eng*. 2020;77:103241.
87. Majidi R, Edwards S, Zhang J, Sant R, Last N. Drilling depleted sands: Geomechanics, challenges and mitigations. In: *SPE Annual Technical Conference and Exhibition*. Society of Petroleum Engineers; 2015 September..
88. Meng M, Baldino S, Miska SZ, Takach N. Wellbore stability in naturally fractured formations featuring dual-porosity/single-permeability and finite radial fluid discharge. *J Petrol Sci Eng*. 2018.
89. Cayeux E, Daireaux B. Insights into the physical phenomena that influence automatic gain/loss detection during drilling operations. *SPE Drill Complet*. 2016;32(01):13–24.
90. Cayeux E, Daireaux B. Precise gain and loss detection using a transient hydraulic model of the return flow to the pit. In: *SPE/IADC Middle East Drilling Technology Conference & Exhibition*. Society of Petroleum Engineers; 2013.
91. Easton MDJ, Nichols J, Riley GJ. Optimizing hole cleaning by application of a pressure while drilling tool. In: *SPE/IADC Conference*. Society of Petroleum Engineers; 1997.
92. Hutchinson M, Rezmer-Cooper I. Using downhole annular pressure measurements to anticipate drilling problems. In: *SPE Annual Technical Conference and Exhibition*. Society of Petroleum Engineers; 1998.
93. Mallary CR, Varco M, Quinn DA. Using pressure-while-drilling measurements to solve extended-reach drilling problems on alaska's north slope. In: *SPE Western Regional Meeting*. Society of Petroleum Engineers; 1999 January.
94. Roy S, Zamora M, Froitland TS. Surge/swab considerations in deepwater drilling. In: *AADE Annual Technical Forum, Houston TX*, 1999.
95. Zamora M, Roy S. Using true real-time data interpretation to facilitate deepwater drilling. In: *AADE Annual Technical Forum, Houston, TX*, 2001.
96. Roy S, Power D. Using real-time hydraulics modeling to complement annular-pressure-while-drilling data. In *AADE Technical Conference*, 2002.
97. Golwalkar A, Lang CM, Doodraj S, Singh AK, Manoranjan K, Pandita A. Exploratory drilling in severely ballooning formation-use of best drilling practices and real time monitoring for low cost mitigation. In: *International Petroleum Technology Conference*; 2016.
98. Dalton CL, Paulk MD, Bittar M. January. Real-time, time-lapse resistivity logging with a wired composite tubing. In: *SPE International Petroleum Conference and Exhibition in Mexico*. Society of Petroleum Engineers; 2002.
99. Bratton TR, Rezmer-Cooper IM, Desroches J, Gille YE, Li Q, McFayden M. How to diagnose drilling induced fractures in wells drilled with oil-based muds with real-time resistivity and pressure measurements. In: *SPE/IADC Drilling Conference*. Society of Petroleum Engineers; 2001 January.
100. IADC MPD & UBO Committee Meeting Minutes, *IADC Underbalanced Drilling Operations Committee Meeting-1st Quarter, Leiden, The Netherlands*, 2004; 15-16 March.
101. IADC MPD & UBO Committee Meeting Minutes, *IADC Underbalanced Drilling Operations Committee Meeting. Houston, TX*, 2004; 13-14 December.

102. Malloy KP, Stone R, Medley GH, Hannegan DM, Coker OD, Reitsma D, Santos HM, Kinder JI, Eck-Olsen J, McCaskill JW, May JR. Managed-pressure drilling: What it is and what it is not. In: *IADC/SPE Managed Pressure Drilling and Underbalanced Operations Conference & Exhibition*. Society of Petroleum Engineers; 2009 January.
103. Hannegan DM, Wanzer G. Well control considerations-offshore applications of underbalanced drilling technology. In: *SPE/IADC Drilling Conference*. Society of Petroleum Engineers; 2003 January.
104. Aadnøy BS, Cooper I, Miska ZS, Mitchell RF, Payne ML. *Advanced Drilling and Well Technology*. SPE; 2009.
105. Terwogt JH, Mäkiaho LB, Van Beelen N, Gedge BJ, Jenkins J. Pressured mud cap drilling from a semi-submersible drilling rig. In: *SPE/IADC Drilling Conference*. Society of Petroleum Engineers; 2005.
106. Nauduri ASS, Medley GH, Schubert JJ. MPD: Beyond narrow pressure windows. In: *IADC/SPE Managed Pressure Drilling and Underbalanced Operations Conference & Exhibition*. Society of Petroleum Engineers; 2009 January.
107. Tirado Vargas GR, Lupo CPM, Beltran JC, Duno H, Iturrios C, Gallo Zapata JF, Hernandez Franco T, Centeno M. MPD Makes possible to drill and trip out of the hole in a gas well with a combination of a narrow mud weight window and a serious ballooning effect. In: *IADC/SPE Managed Pressure Drilling and Underbalanced Operations Conference & Exhibition*. Society of Petroleum Engineers; 2011.
108. Ochoa Lugo AJ, Acevedo OD, Nieto L, Lambarria JE, Perez H. Successful application of MPD (managed pressure drilling) for prevention, control, and detection of borehole ballooning in tight gas reservoir in cuervito field, Mexico. In: *Canadian Unconventional Resources Conference*. Society of Petroleum Engineers; 2011.
109. Loux F, Bunyak MJ, Kongpat N, Pattanapong K, Eagark P, Rubianto I, Gallo F, Intravichit J, Charnvit K, Prasetia AE, Houng NH. Managed pressure drilling significantly reduces drilling costs on extremely challenging ultra HT wells in the Gulf of Thailand. In: *SPE/IATMI Asia Pacific Oil & Gas Conference and Exhibition*. Society of Petroleum Engineers; 2015.
110. Hernandez J, Arnone M, Callison R, Shirley G. Recovering the confidence to drill in a field after dealing with a blowout, the managed pressure drilling approach. Operator finds an effective way to address the high potential for blowouts and drilling challenges in a field in utah. In: *SPE Eastern Regional Meeting*. Society of Petroleum Engineers; 2014.
111. Medina L, Baker J, Markabi M, Rojas J, Tarique Z, Dow B. Automated MPD and an engineered solution: A case history in western Canada. In: *IADC/SPE Drilling Conference and Exhibition*. Society of Petroleum Engineers; 2014.
112. Sharma D, Agarwal C, Lobo M, Chakraborty B, Brickell N, Pathak M, Lang C. Use of managed pressure drilling technology helped in achieving well objectives: A case study of an offshore HTHP well in India. In: *SPE/IADC Managed Pressure Drilling and Underbalanced Operations Conference & Exhibition*. Society of Petroleum Engineers; 2015.
113. Barbosa A, Gallego G, Clemente F, Padilla R, Mondragón GEG, Balderas JA. Automated MPD system in offshore gulf of Mexico further substantiates value of drilling technique in high-pressure zones. In: *SPE Latin America and Caribbean Petroleum Engineering Conference*. Society of Petroleum Engineers; 2017.
114. Rosenberg SM, Gala DMM. Liner drilling technology as a tool to reduce NPT-gulf of Mexico experiences. In: *SPE Annual Technical Conference and Exhibition*. Society of Petroleum Engineers; 2011.
115. Fontenot K, Strickler RD, Molina P. Improved wellbore stability achieved with Casing Drilling operations through drilling fluids. In: *Smear Effect, paper WOCWD-0431-04, presented at 2004 World Oil Casing While Drilling Technical Conference, Houston, TX*, 2004.
116. Marbun BT, Widiyanto YA, Kurnianto BE. Feasibility study of casing while drilling application on geothermal drilling operation. In *Thirty-Ninth Workshop on Geothermal Reservoir Engineering, Stanford, California*, 2014; February.
117. Terrazas Romero M, Estrada Garcia M, Lopez-Solis V, Jardines Tena A, Diaz E, Fisher M. Drilling with liner on horizontal oil wells. In: *SPE/IADC Drilling Conference*. Society of Petroleum Engineers.; 2007.
118. Rosenberg SM, Gala DM, Xu WJ. Liner drilling technology as a mitigation to hole instability and loss intervals: A case study in the gulf of Mexico. In: *IADC/SPE Drilling Conference and Exhibition*. Society of Petroleum Engineers; 2010.
119. Rosenberg SM, Gala DMM. Liner drilling technology as a mitigation to wellbore ballooning - a successful case study in the gulf of Mexico shelf. In: *SPE/IADC Drilling Conference and Exhibition*. Society of Petroleum Engineers; 2011.